

**A 258-Year Record of Precipitation as Snow from Tree-rings,
Southern Coast Mountains, British Columbia**

by

Stuart James MacKinnon

Honours Bachelor of Science, University of British Columbia, 2011

Bachelor of Education, University of British Columbia, 2012

A Thesis Submitted in Partial Fulfillment of the
Requirements for the Degree of

MASTER OF SCIENCE

in the Department of Geography

© Stuart James MacKinnon, 2016
University of Victoria

All rights reserved. This thesis may not be reproduced in whole or in part, by photocopy
or other means, without the permission of the author.

SUPERVISORY COMMITTEE

A 258-Year Record of Precipitation as Snow from Tree-rings,
Southern Coast Mountains, British Columbia

by

Stuart James MacKinnon

Honours Bachelor of Science, University of British Columbia, 2011

Bachelor of Education, University of British Columbia, 2012

Supervisory Committee

Dr. Dan J. Smith (Department of Geography)

Supervisor

Dr. Terry D. Prowse (Department of Geography)

Departmental Member

Dr. Bethany L. Coulthard (The University of Arizona)

Additional Member

ABSTRACT

Supervisory Committee

Dr. Dan J. Smith (Department of Geography)

Supervisor

Dr. Terry D. Prowse (Department of Geography)

Departmental Member

Dr. Bethany L. Coulthard (The University of Arizona)

Additional Member

In Pacific North America, a substantial amount of the streamflow available during the dry summer months originates from melting mountain snowpacks. Since the start of the twenty-first century, these mountain snowpacks have been declining due to the impacts of global climate change and could have severe implications for future water availability in many regions. To develop robust predictive models of future water availability derived from mountainous snowpacks, the longest possible data record is required. However, instrumental data for snow measurements, when available, are limited to a length of only five or six decades in most regions of Pacific North America. In this study, tree-rings from snow-depth sensitive tree species (mountain hemlock (*Tsuga mertensiana* (Bong.) Carrière) and subalpine fir (*Abies lasiocarpa* (Hook.) Nutt.)) were used as a proxy to develop a 258-year record of precipitation as snow (PAS) for the southern Coast Mountains of British Columbia. Four snow models were evaluated based on a suite of dendroclimatological model diagnostics. From these, one PAS reconstruction was carried out. The reconstruction was unable to properly validate using the leave-one-out cross validation method. This result is attributed to the combination of a short calibration period, a potentially weak climate signal, and the absence of signal enhancement. Despite this outcome the research resulted in number of inferences and recommendations useful for future research.

TABLE OF CONTENTS

SUPERVISORY COMMITTEE	ii
ABSTRACT	iii
TABLE OF CONTENTS	iv
LIST OF TABLES	vi
LIST OF FIGURES	vii
ACKNOWLEDGEMENTS	viii
CHAPTER 1: INTRODUCTION	1
1.1 Introduction	1
1.2 Research Goals and Objectives	3
1.3 Thesis Structure	3
CHAPTER 2: LITERATURE REVIEW	4
2.1 Climatic Drivers and their Influence on Mountain Snowpacks	4
2.2 Dendroclimatology	7
2.3 Dendrohydrology and Snowpack Reconstruction	9
2.4 Related Local Dendroclimatological Research	13
CHAPTER 3: STUDY AREA AND DATA	16
3.1 Study Area	16
3.2 Tree-ring Sampling Sites	18
3.3 Hydroclimatic Data	20
CHAPTER 4: SNOW RECONSTRUCTIONS	22
4.1 Tree-ring Chronologies and Correlation Analysis	22
4.2 SWE Reconstruction	28

4.3 PAS Reconstruction	30
CHAPTER 5: DISCUSSION	37
5.1 Interpretation	37
5.2 Historical Trends in the Snowpack History	38
5.3 Reconstruction Comparisons	40
5.4 Difficulties Associated with a Snowpack Reconstruction	43
CHAPTER 6: CONCLUSIONS	46
6.1 Introduction	46
6.2 Thesis Summary	46
6.3 Conclusion	48
6.4 Recommendations for Future Research	48
REFERENCES	50

LIST OF TABLES

Table 3.1: Tree-ring sample site locations and sampling information.	19
Table 3.2: Tree-ring chronology information.	20
Table 3.3: Hydroclimatic station location data.	21
Table 4.1: Overview of the multiple regression analysis for the two best SWE models.	28
Table 4.2: LOO cross-validation analysis for the two SWE models	28
Table 4.3: Overview of the multiple regression analysis for the two best PAS models.	30
Table 4.4: LOO cross-validation analysis for the two PAS models	30

LIST OF FIGURES

Figure 3.1: Map of the southern Coast Mountain region showing the location of the five study sites.	16
Figure 4.1: Correlation matrices with Pearson's r values for the Lightning Lakes SWE snow data and the seven residual tree-ring chronologies.	24
Figure 4.2: Correlation matrices with Pearson's r values for the Lightning Lakes SWE snow data and the seven arstan tree-ring chronologies.	25
Figure 4.3: Correlation matrices with Pearson's r values for the Mt. Cheam PAS snow data and the seven residual tree-ring chronologies.	26
Figure 4.4: Correlation matrices with Pearson's r values for the Mt. Cheam PAS snow data and the seven arstan tree-ring chronologies.	27
Figure 4.5: Line graph showing the observed SWE compared with results from the LOO cross-validation procedure of both models.	29
Figure 4.6: Line graph depicting the closeness of the calibration and validation datasets for the LOO cross-validation of PAS model #2.	32
Figure 4.7: PAS reconstruction (dark line) over top of the confidence intervals associated with the reconstruction.	33
Figure 4.8: PAS reconstruction represented as a deviation from the mean annual observed PAS value.	34
Figure 4.9: PAS reconstruction (blue line) with the five-year running mean (red line) overlain to highlight possible cyclical patterns.	35
Figure 4.10: PAS reconstruction (blue line) with the eleven-year running mean (red line) overlain.	36
Figure 5.1: Line graph comparing the PAS reconstruction from this research study to the Tatlayoko SWE reconstruction completed by Starheim et al. (2013)	41
Figure 5.2: Line graph comparing the PAS reconstruction from this research study to the Mt. Cronin SWE reconstruction completed by Starheim et al. (2013)	42

ACKNOWLEDGEMENTS

I would like to start by acknowledging the tremendous amount of help and support that was provided by my committee members: Drs. Dan Smith, Terry Prowse and Bethany Coulthard. Without the guidance from these three individuals I would never have been able to get to this point and complete my thesis. Next, I would like to acknowledge and thank my wife, Angelia, for being there for me when I needed her most. Lastly, I would like to thank all my family and friends for your support and assistance on this educational journey.

CHAPTER ONE: INTRODUCTION

1.1 Introduction

In Pacific North America multiple large-scale climate systems, as described by the Pacific Decadal Oscillation (PDO), Southern Oscillation Index (SOI) and the Pacific North American (PNA) pressure anomaly, significantly impact the terrestrial surface climate and hydrology (Starheim et al., 2013; Whitfield et al., 2010). Over the last century, long-term changes in the behaviour of these climate systems have resulted in unprecedented declines in seasonal runoff from snow, which have affected the availability of water during the summer months (Barnett et al., 2005; Mote et al., 2005; Pederson et al., 2011).

Snowpack development varies from year to year; however, the impacts from climate change are becoming more apparent. It should be noted that an overall snowpack decline does not mean that all regions are experiencing lower annual snowpacks. Instead, with increasing temperatures, snowpacks at mid-elevations have a shorter duration to develop and tend to melt earlier in the year, while high-elevation regions are largely unaffected or even experience greater winter precipitation (Pederson et al., 2013; Stewart, 2009). In southern British Columbia above average snowpacks developed during the period from 1966-1976, whereas from 1976-1992, below average snowpacks were more common. This temporal difference in snow accumulation appears to be related to positive and negative phases of the PDO (Gedalof and Smith, 2001; Moore and McKendry, 1996).

Snow water equivalent (SWE), a measure of the amount of water in a snowpack, can provide researchers with many insights into annual, decadal and longer climatic patterns. However, a number of factors influencing a snowpack can complicate analysis of the contributions from climatic patterns. These variables include parameters such as the amount of

winter snow loss from snowmelt, ablation, interception and redistribution. Of particular concern is the short length of available snowpack data, which are typically limited to the last half a century. For more accurate future projections of the amount of water contained within seasonal snowpacks, it is necessary to extend the historic snow data.

To establish long-term records of natural SWE fluctuation, it is critical to have a long duration of climate data to work with. The use of tree-rings as a snow proxy can allow for the extension of annual or seasonal snow records (Larocque and Smith, 2005). In specific environments, trees indicate climate information, especially extreme events, in their ring widths (Littell et al., 2008; Loaiciga et al., 1993).

Dendroclimatology, the use of trees to reconstruct climate information, has proven successful for many climate reconstruction applications including temperature, streamflow and snowpack (Flower and Smith, 2011; Hart et al., 2010; Woodhouse, 2003). For some high-elevation tree species growing in the Pacific Northwest, total annual snowpack depth and summer temperature are the two primary factors influencing radial growth. Snow is especially influential in coastal regions with deep snowpacks that need to melt before the annual growth can begin (Graumlich and Brubaker, 1986; Larocque and Smith, 2005; Laroque and Smith, 2005; Marcinkowski et al., 2015; Peterson and Peterson, 1994). Data from these trees can, in some circumstances, be used to reconstruct snow-related variables, either SWE or precipitation as snow (PAS). Snow and snow-meltwater reconstructions have previously been developed in this region by Coulthard, Hart and Starheim (Coulthard 2015; Coulthard and Smith, 2015; Coulthard et al., 2016; Hart et al., 2010; Starheim et al., 2013).

1.2 Research Goals and Objectives

This research attempted to use tree-ring chronologies to reconstruct proxy SWE and PAS records for the southern British Columbia Coast Mountain region. Two primary goals underlie the research: 1) to document and analyze historical trends in snowpacks and the associated climatic patterns controlling these trends; and, 2) to develop long-term SWE and/or PAS reconstructions based upon mountain hemlock and subalpine fir tree-ring chronologies collected in the southern Coast Mountains. Specific objectives were to:

1. describe trends and identify drivers of long-term change in snowpack variability;
2. construct proxy records of SWE and PAS for the duration of the tree-ring record using mountain hemlock and subalpine fir tree-ring chronologies;
3. review, examine and describe trends in the reconstructed proxy records of SWE and PAS.

1.3 Thesis Structure

The thesis consists of six chapters. Chapter One introduces the research, summarizes current research gaps, and discusses the purpose and objectives of the thesis. Chapter Two presents a literature review that reviews: climatic drivers and their influence on mountain snowpacks, dendroclimatology, and dendrohydrology and snowpack reconstructions. Chapter Three describes the study area and reviews the data used in the research project. Chapter Four details the methods used for the development of the snow (SWE and PAS) reconstructions, summarizes the results from the reconstructions, and explains the associated analyses that were carried out. Chapter Five interprets the results of the research, presents a discussion of the project in the context of similar research that has been completed, and explains the difficulties associated with performing a snowpack reconstruction. Chapter Six concludes the thesis by summarizing the research findings, providing concluding comments, and identifying future research options.

CHAPTER TWO: LITERATURE REVIEW

2.1 Climatic Drivers and their Influence on Mountain Snowpacks

In Spring 2015, record-breaking low snowpack totals in Pacific North America (PNA) were recorded at snow survey stations from California to British Columbia (BC). The significance of this event was emphasized by Belmecheri et al. (2015) who reported that the April 1, 2015, Sierra Nevada Mountain snowpack was the lowest in 500 years. In a region increasingly dependent upon the melting of mountain snowpacks for summer stream discharge, the implications for water security were severe (Barnett et al., 2005).

As the climate of the Earth warms more precipitation will fall as rain rather than snow and result in reduced seasonal snowpacks. Globally the spring snowmelt period is expected to begin earlier in most temperate regions (Barnett et al., 2005). Overall, the decreased snowpack accumulation will result in less water from melting snowpacks during the summer months when water resources are already the most stressed (Barnett et al., 2005). Although the magnitude of future snowpack decline remains uncertain, it is evident that a warming climate is going to have an impact on water availability in regions where the annual water supply is dependent upon snow precipitation (Barnett et al., 2005; Pederson et al., 2011).

In PNA mountain snowpacks serve as a cold-season reservoir for water storage that releases water during the warmer summer months to dry and hot lower elevation valleys (Stewart, 2009). In many snowmelt-fed valleys across the globe, there is sufficient local precipitation during the fall, winter, and spring months. There is, however, often insufficient water supplied during the summer months to meet local needs. This water supply deficit has historically been compensated for by water originating due to snowmelt in high elevation regions of the watershed (Mote et al., 2005). The issue for most water managers is that with smaller

snowpacks and an earlier onset of the spring snowmelt, the summer stream discharge typically provided by the high mountain snowmelt will decrease progressively over time. When considered in conjunction with increases in the local summer drought conditions associated with the climate change induced temperature increases, the reduced water availability from headwater mountain watersheds could be extremely problematic for downstream communities. The problems currently being faced by people living in regions such as California are only the beginning (Belmecheri et al., 2015; Woodhouse et al., 2010).

In PNA, mountain watersheds within the western continental USA and southern BC have already experienced an earlier onset of the spring melt period and overall lower summer stream discharges (Stewart, 2009). In contrast, some regions in northern BC and Alaska have experienced deeper winter snowpacks due to the increased temperatures and associated increased winter precipitation (McCabe and Clark, 2005; Mote, 2003a; Nijssen et al., 2001; Stewart, 2009). Although noteworthy, the changes in northern BC and Alaska will not be explored further as this research focuses on southwestern BC; therefore, the most relevant research comes from this region and nearby Washington State.

The onset of the snowmelt period has already shifted one to four weeks earlier in much of western North America, with trends toward an earlier snowmelt onset in the near future (Stewart et al., 2005). Just as the change in timing of snowmelt onset varies in the region based on location, the magnitude of snowpack decline (i.e., April 1 Snow Water Equivalent) is related to the specific location (Mote, 2003b; Pederson et al., 2013). Local variations in both snowpack declines and an earlier onset of snowmelt have been shown to be consistent with elevation and latitude based warming trends (Mote et al., 2005).

The major question remaining to be answered is: what is driving these snowpack shifts? Consideration needs to be made for the cyclical climatic patterns that affect PNA and yearly snowpacks. Of particular importance are synoptic weather patterns described by the Pacific Decadal Oscillation (PDO) and El Niño/Southern Oscillation (ENSO) (Chapman, 2007; Whitfield et al., 2010). While weather patterns are more variable than long term climatic patterns, exploring trends over time is important for understanding climate change. The PDO is a long-term cyclical climatic driver that shifts from “cool” to “warm” phases; however, neither the duration nor the mechanism behind these shifts are clear (Mantua and Hare, 2002). It appears that there have been eleven PDO shifts since 1650 A.D., which averages one shift every 23 years (Gedalof and Smith, 2001). Nonetheless, such predictions can be quite challenging in part due to the highly varied duration of the PDO phases. ENSO effects are better understood and follow a more predictable cycle than those of the PDO (Whitfield et al., 2010). Whether derived from PDO or ENSO, periods of “cool” and “warm” events have either positive or negative effects on the depth of snowpack developed, respectively. These cyclical climatic patterns need to be considered and accounted for before trying to accurately determine the degree of change in snowfall caused by climate change.

To what degree climate change will affect regional snowpacks in the future remains uncertain. It is evident, however, that diminished mid-latitude snowpacks are likely and consequently some regions will experience decreased water availability during summer months (Barnett et al., 2005; Woodhouse et al., 2010). Snow-dominated watersheds in the mid-latitudes (as opposed to polar regions) are projected to be impacted more by a changing climate. Although local changes are relatively small on average and typically constrained to mountain ranges, the total area and water contained within mid-latitude snowpacks is substantial (Nijssen et al., 2001).

In addition to there being reductions in the seasonality and quantity of runoff from smaller mountain snowpacks, these reduced snowpacks may result in a more rapid increase in global temperature. Snow generally has a high albedo or reflection coefficient, and therefore, reflects substantially more light and provides more insulation than other surfaces (e.g., forest, desert, grassland, and pavement). Therefore, persistent snow cover has an important temperature moderating effect (Stewart, 2009). Reductions in the total area of snow cover across the globe will reduce the amount of short wave radiation reflected back to space, and thus further accelerate the future rate of global temperature increase.

Long-term climate information, and in particular snowpack data, has been limited at high elevation temperate locations due to the large degree of spatial variability that exists in these locations. In addition, instrumental snowpack data are mainly constrained to the last five or six decades, reducing their reliability for long-term climatic projections (Woodhouse, 2003).

2.2 Dendroclimatology

Dendroclimatology is based on the understanding that the yearly radial increment of a tree ring is a growth response to annual climatological and environmental conditions (Nelson et al., 2011). For example, in the temperate mid-latitudes trees often respond to changes in temperature, with distinct annual seasonality. In these settings simple linear relationships between radial tree-ring growth data and temperature data allow for robust proxy reconstructions of temperature. For instance, in northwestern BC the radial growth of white spruce was shown to be strongly correlated to mean June-July temperatures, and this relationship allowed for the reconstruction of a June-July temperature record to 1772 A.D. (Flower and Smith, 2011).

The annual radial growth of many high-elevation tree species in PNA is limited by one or two dominant environmental variables. In the Mountain Hemlock biogeoclimatic Zone (MHZ)

the climatic variables that tend to be most important are either summer temperature (i.e., July temperature) or the duration of the growing season, generally equivalent to the number of days that the ground remains snow-free (Laroque and Smith, 2005). While one or two climatic variables often explain the majority of annual radial growth (i.e., growing season and July temperature), in some situations discerning tree growth-climate relationships is not easily accomplished. It is not uncommon to see tree-ring records demonstrating a sensitivity to numerous climate parameters, and for these to be combined to create a more robust reconstruction than use of a single climate variable allows for (Laroque and Smith, 1999; Larocque and Smith, 2005). For robust reconstructions, it is important to ensure that sufficient model predictors are used to explain variance in the predictand (i.e., snow) data, while also confirming that the model is not over-fit (Stokes and Smiley, 1968).

Tree-ring chronologies can be used to extend instrumental climate data into the past, with the duration of the proxy record determined by the age and climate sensitivity of trees in the study area. Temperate subalpine forests are typically found where summer temperatures are cool, winters are severe, and the onset of snowmelt is delayed; all of which results in limited establishment, growth and survival of even the most adapted tree species (Antos and Parish, 2002; Peterson and Peterson, 1994; Peterson and Peterson, 2001). The survival challenges for tree species in cold subalpine environments are confounded by associated canopy damage including: wind breakage, snow and ice damage, and in some cases, limb breakage (Grier 1988).

2.3 Dendrohydrology and Snowpack Reconstruction

Dendrohydrology seeks to use radial growth data to hindcast a proxy hydrologic variable, based on a statistical relationship between the two. Example target variables include: instrumental streamflow records, precipitation, snow, and other moisture-related variables (Loaiciga et al., 1993; Cleaveland, 2000; Meko et al., 2001; Woodhouse and Lukas, 2006; Hart et al., 2010). These relationships are often associated with particularly wet or dry growing seasons that influence both the hydrologic variable and radial growth (Loaiciga et al., 1993; Lutz et al., 2012). In cold temperate regions, these relationships are complicated as deep seasonal snowpacks frequently melt in the late spring to early summer period, influencing the amount and timing of water availability for tree growth, and ultimately the length of the growing season (Coulthard, 2015; Lutz et al., 2012; Starheim et al., 2013). Thus, in regions where snow delays the onset of radial growth, developing a proxy snow history is possible because of the negative linear relationship between radial growth and snow (Hart et al., 2010; Starheim et al., 2013).

Seasonal snowpacks, measured as snow water equivalent (SWE), in much of PNA have been declining over the past 30-50 years resulting in increasing attention given to understanding whether these changes are due to multi-decadal climate fluctuations or globally warming climates (Masiokas et al., 2012; Pederson et al., 2011; Starheim et al., 2013). Recent dendrohydrological-derived snow histories in mountainous regions (i.e., Pacific USA, Chile, India) are providing the insights essential for understanding the significance of such snowpack declines (Anderson et al., 2012; Masiokas et al., 2012; Pederson et al., 2011; Timilsena and Piechota, 2008; Woodhouse, 2003; Yadav and Bhutiyani, 2013).

There have been a number of notable tree ring-derived snowpack reconstructions completed to date (Anderson et al., 2012; Masiokas et al., 2012; Pederson et al., 2011; Timilsena

and Piechota, 2008; Woodhouse, 2003; Yadav and Bhutiyani, 2013). All the studies compared regionalized SWE data to either water-limited or snow-restricted tree-ring chronologies to derive multi-century proxy snow records (Coulthard, 2015; Coulthard and Smith, 2015; Coulthard et al. 2016; Marcinkowski et al., 2015; Starheim et al., 2013; Watson and Luckman, 2016). The studies are discussed in detail below, with the key points related to the thesis research presented in the final section of the literature review.

The first attempt at a dendrochronologically-derived snowpack reconstruction was completed for the Gunnison River basin in the western reaches of Colorado, USA (Woodhouse 2003). Prior to this study, researchers had simply noted that the radial growth of some high elevation trees was related to the depth of the seasonal snowpack (i.e., Peterson and Peterson 1994). Expanding upon these observations, Woodhouse (2003) collated April 1 SWE data from 19 snow course stations to provide a temporal range of snowpack variation from 1942 to 1990. Six established tree-ring chronologies were utilized and nine new ones were developed during this study (Woodhouse, 2003). The fifteen chronologies were entered into a stepwise multiple regression to simulate the instrumental SWE data. The four predictor chronologies used in the reconstruction were all located outside of the river basin itself (Woodhouse, 2003). Once the regression analysis was completed, the model underwent a split-sample calibration and verification scheme that involved using a model generated from the first half of the data set to generate the second half of the data set, and vice versa (Meko et al., 2001; Woodhouse, 2003). The model passed both the calibration and verification procedures, and the April 1 SWE reconstruction explained 63% of the variance in the instrumental record. This reconstruction model was used to extend the historical snowpack data to the year 1569, thereby producing a 431-year reconstruction (Woodhouse, 2003). Woodhouse (2003) did note that although SWE

reconstructions appeared to follow the typical dendrochronology pattern; in general, reconstructions from tree-ring chronologies tend to be conservative estimates of the instrumental data they are trying to recreate.

Timilsena and Piechota (2008) expanded upon the analyses of Woodhouse (2003). Where Woodhouse (2003) examined only one river basin in the eastern region of the upper Colorado River Basin (UCRB), Timilsena and Piechota (2008) developed a regional SWE reconstruction. The UCRB was re-examined using 40 snow course stations and partial least square regression (PLSR). A statistically modified principle component analysis (PCA) regionalized April 1 SWE value was developed. The regionalized SWE value was then used with residual tree-ring chronologies to generate regional composite SWE values for three of the four PCA vectors of the UCRB; the east, west, and south. An attempt to develop a reconstruction model for the north vector was not successful as the tree-ring chronologies were inadequately correlated with the SWE data (Timilsena and Piechota, 2008). The SWE reconstruction explained 61% of the variance in the east, 44% of the variance in the west, and 58% of the variance in the south. Although the statistical strength of these reconstructions were not high, they did allow the researchers to examine historic trends in local droughts (Timilsena and Piechota, 2008).

Anderson et al. (2012) undertook an additional SWE reconstruction within the UCRB that specifically examined the influence of the PDO and Southern Oscillation Index (SOI) on the SWE reconstruction in an effort to further increase the modelling robustness of a snowpack reconstruction. They utilized the same SWE data and 50 tree-ring chronologies, 44 of which were previously used by Timilsena and Piechota (2008). Unlike Timilsena and Piechota (2008), Anderson et al. (2012) used a stepwise multiple linear regression to develop the model and a leave-one-out cross-validation approach. The novel aspect of this study came from the inclusion

of climate signal variables as predictand variables within the regression analysis; particularly the impact of the PDO and SOI (Anderson et al., 2012). Following their analyses, the SOI variable was deemed statistically relevant but the PDO variable rejected. Through the use of SOI as a model predictand, the three previously successful PCA vectors were more robust and the north region was successfully reconstructed (Anderson et al., 2012). The study verified the importance of accounting for normal cyclical climatic variability in SWE reconstructions.

Pederson et al. (2011) compiled 66 tree-ring chronologies to represent key runoff locales for the Colorado, Columbia, and Missouri rivers, along with highly regionalized SWE data-sets based on approximately 40,000 km² units (Pederson et al., 2011). From the data-sets, they were able to recreate 27 statistically relevant composite snowpack reconstructions. Their analysis of these snowpack reconstructions was able to address some regional questions about historical snowpack, and provide insight into the long term trends in snowpack for the western USA.

Masiokas et al. (2012) used tree-ring, SWE and streamflow data-sets to perform two snowpack reconstructions for a region of the Chilean Andes. Tree-ring chronologies along with SWE data were used to reconstruct the snowpack to AD 1150, and streamflow data was used with the SWE data to reconstruct a snowpack record back 150 years (Masiokas et al., 2012). Both reconstructions were based on a simple regression for the model, and were validated via leave-one-out cross-validation. The tree-ring based reconstruction explained 45% of the variance and was reported to perform poorly during high snow depth years. The streamflow based reconstruction deemed statistically robust, explaining 84% of the variance, and appeared to follow year-to-year fluxes closely (Masiokas et al., 2012).

Yadaz and Bhutiyani (2013) completed a snowpack reconstruction in the Himalaya Mountains, India. Their study was constrained by the available data-sets, with only 22 years of

SWE data and six tree-ring chronologies. The researchers utilized a PCA regression similar to that employed by Timilsena and Piechota (2008) to generate a reconstruction model validated using the leave-one-out cross-validation method (Yadaz and Bhutiyani, 2013). Due to the limited nature of the available snowpack data, Yadaz and Bhutiyani (2013) performed independent verifications using local precipitation data and other available historic information to review the validity of the reconstruction.

In most of the subalpine temperate regions of Eurasia and North America, warming climates have impacted the amount of snowfall and the timing of snowmelt, which in turn has implications for radial tree growth at these locations (D'Arrigo et al., 2004; Vaganov et al., 1999). Generally, there seems to have been an overall increase in radial tree growth, likely due to the lengthened interval between the end of the snowmelt period and the onset of snowfall in the fall. This trend is not, however, consistent in all regions. For example, trees at the altitudinal treeline are actually experiencing declines in annual radial growth, likely due to an increase in winter precipitation and therefore deeper seasonal snowpacks (D'Arrigo et al., 2004). Vaganov et al. (1999) found that the warming climate did indeed produce more winter precipitation and the onset of snowmelt was later in many parts of sub-arctic Eurasia.

2.4 Related Local Dendroclimatological Research

Six recent studies completed within the coastal mountains of southern BC, Canada and Washington, USA, offer insights relevant to the thesis research (Coulthard, 2015; Coulthard and Smith, 2015; Coulthard et al. 2016; Marcinkowski et al., 2015; Starheim et al., 2013; Watson and Luckman, 2016).

Starheim (2013) examined the July-August runoff for the Skeena and Atnarko Rivers, two nival-reime rivers in west central BC. In addition to these streamflow reconstructions, two

mean summer temperature reconstructions and two end-of winter SWE reconstructions were completed as part of the research project (Starheim et al., 2013). Comparisons of the July-August stream discharge reconstructions with both the summer temperature and SWE reconstructions allowed for the creation of a more detailed picture of the entire runoff dynamics for this region of west central BC (Starheim et al., 2013).

Coulthard (2015), Coulthard and Smith (2015), and Coulthard et al. (2016) studied different dendrohydrological aspects of snow-dominated watersheds on Vancouver Island, BC. They examined conifer trees that were energy-limited by the timing of spring snowmelt, and completed local and regional reconstructions of summer stream discharge based on snowmelt runoff. The snowmelt runoff was based on reconstructed SWE predictands, and the summer streamflow data was most highly correlated with the same year SWE data (Coulthard and Smith, 2015; Coulthard et al. 2016). The summer streamflow reconstructions were used to assess historical drought severity (Coulthard and Smith, 2015). Coulthard (2015) used the same energy-limited conifer trees to develop a reconstruction model that provided a long-term proxy SWE record for Forbidden Plateau, Vancouver Island, that was able to explain 56% of the instrumental data variance (Coulthard, 2015).

An assumption when completing a dendroclimatological reconstruction is that there is a stationary response of tree-ring radial growth to the utilized climate variables; however, it appears that there may be divergence (i.e., a nonstationary response) in the climate-growth response of mountain hemlock trees within the North Cascade Range of Washington, USA (Marcinkowski et al., 2015) and on Mount Washington, Vancouver Island, BC (Coulthard, 2015). A divergence in the climate-growth response of the MH in the Pacific Northwest of Canada and the USA is significant because it requires that all dendroclimatological research

being carried out in this region that utilizes MH chronologies and snowpack climate information needs to carefully examine if there is a such a divergence in any data used as the portion of the data that is divergent may be unreliable for reconstruction purposes. Both Coulthard (2015) and Marcinkowski et al. (2015) report that MH tree-ring chronologies in the Pacific Northwest began diverging from the accepted SWE-growth relationship by 2000. This finding suggests that SWE reconstructions extending beyond 2000 using MH in the Pacific Northwest may be unreliable (Coulthard, 2015, Marcinkowski et al., 2015).

Watson and Luckman (2016) completed a comprehensive examination of correlations between SWE and tree-ring chronologies for the entire southern Canadian Cordillera region. Four distinct chronology groupings were discovered, two with positive correlation relationships between SWE and tree-ring chronologies, and two with negative correlation relationships between SWE and tree-ring chronologies (Watson and Luckman, 2016). The two positive correlation relationships were found in dry valleys and the Rocky Mountain Trench, where summer water availability is limited and tree growth responds positively with increased winter precipitation (i.e., increased winter snow depth) (Watson and Luckman, 2016). The two negative correlation relationships were discovered at wet and cool high elevation locations. At locations in southern BC where summer water availability is plentiful (and increased meltwater from deep snowpacks does not positively affect the growth response of the trees), increased winter precipitation (i.e., increased winter snow depth) was found to reduce both the growing season duration and the energy available at the onset of growth. The latter relationship was assumed to be due to the cold-state viscosity of seasonally frozen ground, thereby preventing the instigation of radial growth until after the snowpack melted (Watson and Luckman, 2016).

CHAPTER THREE: STUDY AREA AND DATA

3.1 Study Area

The study area is found within the subalpine Mountain Hemlock (biogeoclimatic) Zone (MHZ) of the southern Coast Mountains, British Columbia (BC) (Figure 3.1). The MHZ is located in the elevational band from 900 to 1800 m asl, between the Coastal Western Hemlock



Figure 3.1: Map of the southern Coast Mountain region showing the location of the five study sites. The five sites (Brandywine Creek, Rutherford Creek, Hurly FSR, Joffre Lake and Mt. Cheam) are all high elevation sites located within the Mountain Hemlock biogeoclimatic Zone.

Zone (0-900 m asl) and the Alpine Tundra Zone (1800 + m asl) (Klinka et al., 1991; BC Ministry of Forests, 1997; Pojar et al., 1987). This region is characterized by a typical maritime mountain climate, consisting of short, cool summers; long, cool and wet winters; and deep annual snowpacks (BC Ministry of Forests, 1997).

Due to the large elevation range encompassed by the subalpine zone in southwestern BC, the vegetation present is strongly influenced by altitude with: i) dense forests of mountain hemlock (*Tsuga mertensiana* (Bong.) Carrière), amabilis fir and yellow-cedar at the lower elevations, and ii) irregular patches of mountain hemlock, subalpine fir (*Abies lasiocarpa* (Hook.) Nutt.) and yellow-cedar near the timberline at higher elevation (BC Ministry of Forests, 1997). Mountain hemlock is a subalpine conifer tree with densely uniform needles and dark reddish-brown bark that typically grow to be no more than 30 metres tall (Parish and Thomson, 1948). Mountain hemlock are present throughout the MHZ as they grow from mid-elevation to the timberline; however, they are often stunted at higher elevations. Subalpine fir is a narrow, medium sized conifer tree with short stiff branches and smooth grey bark that will usually grow 20 to 35 metres tall (Parish and Thomson, 1948).

Within Pacific North America (PNA) mountain hemlock trees are found from Alaska (Lat 60°N) to California (Lat 36°N), where they are largely restricted to snowy windward sites close to the Pacific Ocean coastline (Gedalof and Smith, 2001). Within the BC MHZ, mountain hemlock trees are the dominant species, but they are commonly found associated with subalpine fir, yellow cedar, Pacific silver fir, and lodgepole pine trees (Gedalof and Smith, 2001).

Typically, the deep annual snowpacks that characterize the MHZ have a long snowmelt period and will not be melted until late June, resulting in a relatively short growing season. The annual radial growth of mountain hemlock trees in the MHZ, in particular the upper reaches of this zone

where the trees are at their most stressed growing states, is highly dependent on winter snow conditions, including the timing of snow onset and snowmelt, temperatures, and the size of snowpack depth developed over the winter (Laroque et al., 2001; Yarie, 1980).

Mountain hemlock trees dominate in the MHZ because they are adapted to the cool, wet climate, with poor soil quality, and deep, persistent snowpacks; they are, however, apparently unable to survive at locations where the soil freezes seasonally (Gedalof and Smith, 2001). On an annual basis, mountain hemlock trees typically have a positive radial growth response to summer air temperature, and a negative radial growth response to late-lying seasonal snowpacks (Gedalof and Smith, 2001; Peterson and Peterson, 2001; Pitman and Smith, 2013). The initiation of the radial growing season for mountain hemlock typically corresponds with the end of the snowmelt period, meaning that late-lying snow inhibits tree growth (Coulthard, 2015). Similar to the radial growth behaviour of mountain hemlock, subalpine firs display a negative radial growth response to winter precipitation and spring snowpack depth, although summer temperature may be the most influential factor depending on snowpack dynamics at the study site (Peterson et al., 2002). It is the negative correlation between tree-ring radial growth and snow depth that allows for snow depth based dendroclimatological reconstructions.

3.2 Tree-ring Sampling Sites

The tree-ring chronologies used in this study were sampled at sites located close to Brandywine Creek, Mt. Cheam, Hurley Forest Service Road, Joffre Lake, and Rutherford Creek (Figure 3.1 and Table 3.1). Four sites were located north of Vancouver in the coastal snow-belt near the Whistler ski resort, while a fifth site was located on a mountain ridge near Mt. Cheam, close to Chilliwack in the Fraser River valley.

At each of the five sites, trees were cored according to standard sampling techniques (Stokes and Smiley, 1968). Two cores were extracted at a standard breast height from each tree using a 5.2 mm increment borer and then transported inside of plastic straws back to the University of Victoria Tree-Ring Laboratory (UVTRL) (Coulthard, 2015). The cores were prepared by allowing them to air-dry and then mounted on boards and sanded to a 1200 grit finish (Coulthard, 2015). Once sanded the annual tree-ring widths were measured using a Velmex system, crossdated using the computer software program COFECHA, and site-specific tree-ring chronologies developed using the dplR R package (Coulthard, 2015). In total seven program ARSTAN tree-ring chronologies (Table 3.2) were constructed (outlined and described below). Further descriptions of the chronology detrending and standardization can be found in Coulthard (2015).

Table 3.1: Tree-ring sample site locations and sampling information.

Site name	Site code	Tree species cored	Latitude, Longitude	Elev (m asl)
Brandywine Creek	98H	mountain hemlock	50°06'N, 123°13'W	1670
Mt. Cheam	99H	mountain hemlock	49°10'N, 121°40'W	1720
Mt. Cheam	99H	subalpine fir	49°10'N, 121°40'W	1720
Hurley FSR	HUSAF	subalpine fir	50°35'N, 123°01'W	1320
Joffre Lakes	JLMH	mountain hemlock	50°21'N, 122°29'W	1540
Rutherford Creek	98F	mountain hemlock	50°16'N, 122°53'W	1380

All of the chronologies were derived from a minimum of ten trees, and a minimum series (cores) of twenty. The oldest tree within the chronologies dates to 1592 A.D., however, the longest chronology dated back to 1650 A.D. after each chronology was truncated where the expressed population signal (EPS) registered less than 0.85 (Wigley et al., 1984). For each chronology, two versions were created: a residual chronology and an arstan chronology. Residual chronologies (as “.rsd” in tables and figures) are sometimes used in dendroclimatology

reconstructions because autocorrelation is removed by an auto-regressive model, and an assumption of running a regression model is that there is no auto-correlation. However, there are cases in dendroclimatology where tree-ring chronologies contain climate-related autocorrelation that it is beneficial to retain in the regression model. Arstan chronologies (as “.ars” in tables and figures) retain the pooled (common) autocorrelation, such that each tree ring is determined not only by the current year’s climate (i.e., snow), but also by the climate of the previous year.

Table 3.2: Tree-ring chronology information.

Chronology Name	Period	Truncated Period ^c	Trees, series	r_1^d	Correlation coefficient (r) ^e			
					SWE.rsd	SWE.ars	PAS.rsd	PAS.ars
Brandywine Creek ^a	1666-1998	1720-1998	17, 30	0.672	-.605	-.635	-.528	-.548
Mt. Cheam ^a	1658-1999	1690-1998	19, 31	0.628	-.336	-.258	-.313	-.313
Mt. Cheam ^b	1592-1999	1650-1998	22, 38	0.604	-.495	-.450	-.348	-.284
Hurley FSR ^b	1751-2012	1835-1998	10, 20	0.587	-.468	-.578	-.519	-.529
Joffre Lakes ^a	1711-2012	1740-1998	15, 28	0.607	-.495	-.475	-.531	-.538
Joffre <i>and</i> Cheam ^a	1658-2012	1658-1998	34, 59	0.568	-.493	-.437	-.455	-.467
Rutherford Creek ^a	1701-1998	1730-1998	19, 35	0.630	-.527	-.494	-.388	-.396

^a Mountain hemlock chronology

^b Subalpine fir chronology

^c Length is truncated when the expressed population signal is less than 0.85 (Wigley et al., 1984).

^d Interseries correlation values; calculated using the program ARSTAN

^e Correlation between the chronology and the indicated snow (SWE/PAS) data set

3.3 Hydroclimatic Data

As with any dendroclimatological reconstruction, the goal is to hindcast a target climate variable by using tree-ring chronologies as a proxy. In the case of this snow reconstruction, I evaluated two snow variables: 1) SWE; and, 2) PAS. The SWE dataset is an observed climatic variable that was obtained from manual snow courses and associated calculations; while the PAS dataset was from the climate modeling software program, ClimateWNA (Wang et al., 2012).

This program downscales and extracts monthly PRISM climate data over a 0.5 km² area for any

specific location/site (Wang et al., 2012). This research used both snow variables, although the original goal was to only use the physically measured SWE data. The initial lack of success with the SWE variable alone prompted the case for also examining the PAS data.

A number of snow course locations were considered for extraction of the SWE dataset (outlined in Table 3.2); however, the Lightning Lake snow course data was used in this research because it had the strongest correlations with the seven tree-ring chronologies. The PAS data used came from ClimateWNA and point values of monthly PAS were obtained for each of the study sites beginning from 1901 (Table 3.2). The Mt. Cheam PAS data was ultimately chosen because the strongest correlations were observed between this snow variable and the seven tree-ring chronologies.

Table 3.3: Hydroclimatic station location data. Lightning Lakes (bolded) was ultimately used for the SWE trials, and Mt. Cheam (bolded) was used for the PAS trials.

Station name	ID	Type	Years	Latitude, Longitude	Elev (m asl)
Lightning Lakes	3D02	snow course ^a	1949-2014	49°03'N, 120°51'W	1250
McGillivray Pass	1C05	snow course ^a	1952-2014	50°42'N, 122°37'W	1715
Duffey Lake	1C28	snow course ^a	1978-2014	50°23'N, 122°29'W	1253
Bridge Glacier	1C39	snow course ^a	1995-2014	50°51'N, 123°28'W	1393
Stave Lake	1D08	snow course ^a	1967-2014	49°35'N, 122°19'W	1211
Wahleach Lake	1D09	snow course ^a	1967-2014	49°14'N, 121°35'W	1395
Nahatlatch River	1D10	snow course ^a	1968-2014	49°50'N, 122°04'W	1530
Gallaghan Creek	3A20	snow course ^a	1976-2014	50°08'N, 123°06'W	1009
Mt. Cheam	-	meteorologic ^b	1901-2011	49°10'N, 121°40'W	1720
Brandywine Creek	-	meteorologic ^b	1901-2011	50°06'N, 123°13'W	1670
Hurley FSR	-	meteorologic ^b	1901-2011	50°35'N, 123°01'W	1320
Joffre Lakes	-	meteorologic ^b	1901-2011	50°21'N, 122°29'W	1540
Rutherford Creek	-	meteorologic ^b	1901-2011	50°16'N, 122°53'W	1380

^a snow surveys produced yearly April 1 values for SWE

^b downscaled meteorologic models produced point PAS values

CHAPTER FOUR: SNOW RECONSTRUCTIONS

4.1 Tree-ring Chronologies and Correlation Analysis

Following construction of the seven residual and seven arstan tree-ring chronologies, each was correlated to both SWE and PAS datasets. The correlation coefficients (r values) are summarized previously (Table 3.2), and the results of these correlations are depicted in the correlation matrices (Figures 4.1 through 4.4) on the following pages. As expected, the tree-ring chronologies were all positively correlated with one another, and the snow data (SWE and PAS) were negatively correlated with all of the tree-ring chronologies. The negative correlation between snow and the tree-ring chronologies confirms the finding of previous researchers that annual tree-ring radial growth is inhibited by deep persistent snowpacks and that increased winter snow depth decreases the amount of summer tree growth. The annual tree-ring radial growth for these trees cannot begin until the snow melts and the soil can warm up and lower the soil moisture viscosity. This finding is key to my research because it shows that the mountain hemlock (MH) and subalpine fir (SAF) trees are energy dependent, and not moisture dependent. If these trees were moisture dependent, a deep snowpack should mean more water availability in summer and the correlation relationship between snow and the chronologies would be positive.

All the tree-ring chronologies, except for the Mt. Cheam MH chronologies (residual and arstan), were significantly correlated with the snow data at the 0.01 significance level. Confirming the significance of this relationship was crucial because it provided justification that the predictors were each independently correlated with the predictand data, a finding that was necessary before multiple linear regression analyses could be completed.

To use an arstan chronology for correlation testing, it is typical to adjust the sample size. Due to the exploratory nature of this research and the fact that all of the best models ultimately

failed to validate (described in the next section), the sample size was not adjusted. If any model had validated, I would have performed a sample size adjustment on the arstan chronologies.

The sum of squares of errors (SSE) was calculated for both the calibration and validation components. Then the mean of the SSE was calculated by dividing SSE by the number of years in the calibration period, yielding the mean squared error of validation (MSE) value (Fritts et al., 1990). Next, the root mean squared error of validation (RMSE) was calculated by taking the square root of the MSE value. The change in the RMSE value indicates the degree of variation between calibration and validation (Fritts et al., 1990). The reduction of error (RE) value was calculated by dividing the SSE of validation by the SSE of calibration, and subtracting this number from one (Fritts et al., 1990). The RE value is important because a positive RE is evidence that some predictive skill exists within the model. Conversely, negative RE values suggest that the reconstruction is deemed to have no predictive skill.

The final step in creating a snow reconstruction involved taking the regression equation for any model that passed the tests associated with validation, and using the associated tree-ring chronologies to extend the climatic variable as far in the past as the tree-ring record extends (Stokes and Smiley, 1968). The calibration period of a dendrochronology reconstruction is the period of time where the target climatic variables (SWE and PAS) overlap with the tree-ring chronologies being used, and over which the regression model used for reconstruction is calibrated (Stokes and Smiley, 1968). For the SWE models, the calibration period was 1949-1998, and for the PAS models the calibration period was 1902-1997. Following the resultant snow reconstruction, analyses were carried out to answer the climatic questions posed in the thesis objectives. Analysis of a developed snow reconstruction was only performed on a model

that was either successfully validated during the LOO cross validation process, or failing a successfully validated model, on a model deemed accurate enough to carry out a reconstruction.

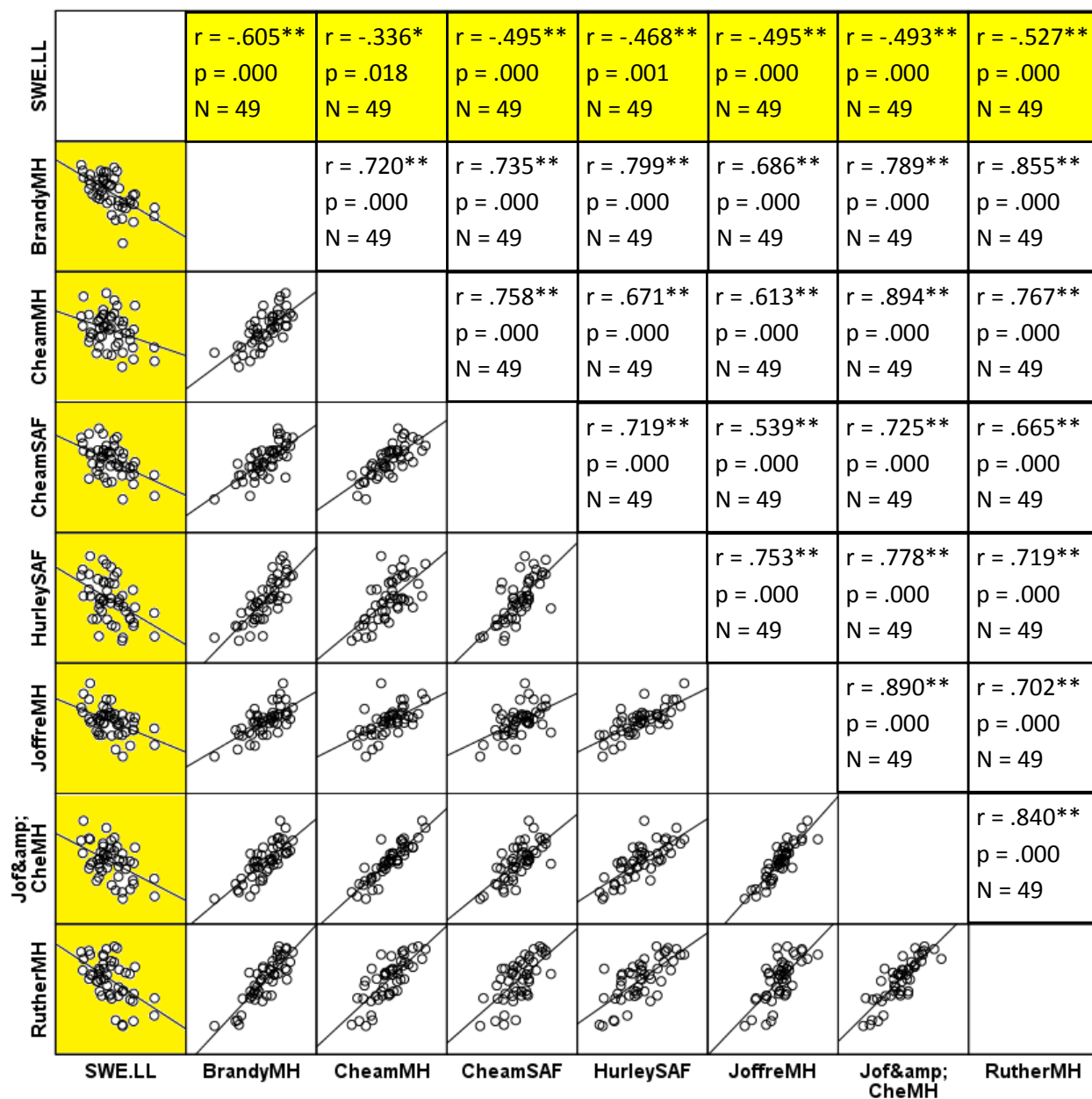


Figure 4.1: Correlation matrices with Pearson's r values for the Lightning Lakes SWE snow data and the seven residual tree-ring chronologies. The yellow highlighted sections of the table display the correlation between SWE and each residual tree-ring chronology individually. A single asterisk (*) indicates significance at the 0.05 level while a double asterisk (**) indicates significance at the 0.01 level.

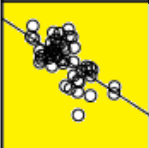
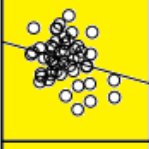
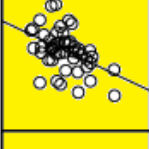
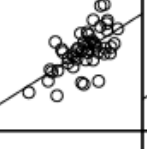
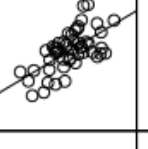
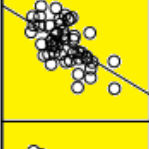
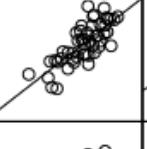
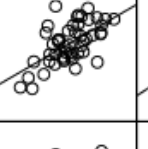
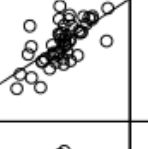
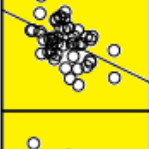
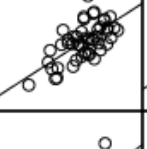
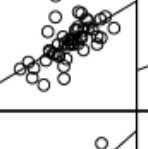
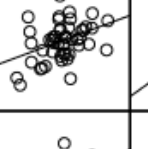
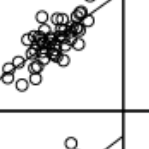
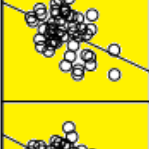
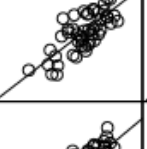
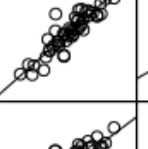
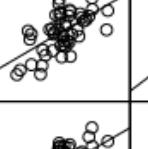
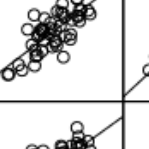
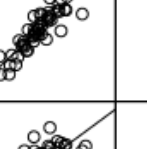
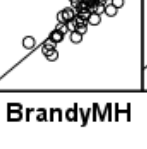
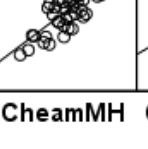
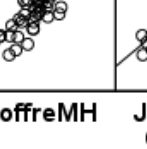
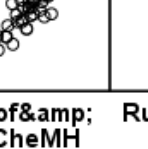
SWE.LL		$r = -.635^{**}$ $p = .000$ $N = 49$	$r = -.258$ $p = .074$ $N = 49$	$r = -.450^{**}$ $p = .001$ $N = 49$	$r = -.578^{**}$ $p = .000$ $N = 49$	$r = -.475^{**}$ $p = .001$ $N = 49$	$r = -.437^{**}$ $p = .002$ $N = 49$	$r = -.494^{**}$ $p = .000$ $N = 49$
BrandyMH			$r = .669^{**}$ $p = .000$ $N = 49$	$r = .623^{**}$ $p = .000$ $N = 49$	$r = .769^{**}$ $p = .000$ $N = 49$	$r = .640^{**}$ $p = .000$ $N = 49$	$r = .742^{**}$ $p = .000$ $N = 49$	$r = .813^{**}$ $p = .000$ $N = 49$
CheamMH				$r = .623^{**}$ $p = .000$ $N = 49$	$r = .608^{**}$ $p = .000$ $N = 49$	$r = .631^{**}$ $p = .000$ $N = 49$	$r = .903^{**}$ $p = .000$ $N = 49$	$r = .780^{**}$ $p = .000$ $N = 49$
CheamSAF					$r = .656^{**}$ $p = .000$ $N = 49$	$r = .375^{**}$ $p = .008$ $N = 49$	$r = .572^{**}$ $p = .000$ $N = 49$	$r = .570^{**}$ $p = .000$ $N = 49$
HurleySAF						$r = .722^{**}$ $p = .000$ $N = 49$	$r = .741^{**}$ $p = .000$ $N = 49$	$r = .711^{**}$ $p = .000$ $N = 49$
JoffreMH							$r = .893^{**}$ $p = .000$ $N = 49$	$r = .721^{**}$ $p = .000$ $N = 49$
Jof& CheMH								$r = .846^{**}$ $p = .000$ $N = 49$
RutherMH								
	SWE.LL	BrandyMH	CheamMH	CheamSAF	HurleySAF	JoffreMH	Jof& CheMH	RutherMH

Figure 4.2: Correlation matrices with Pearson's r values for the Lightning Lakes SWE snow data and the seven arstan tree-ring chronologies. The yellow highlighted sections of the table display the correlation between SWE and each arstan tree-ring chronology individually. A single asterisk (*) indicates significance at the 0.05 level while a double asterisk (**) indicates significance at the 0.01 level.

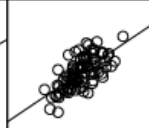
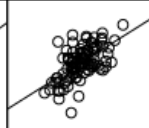
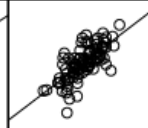
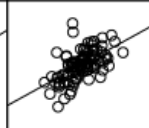
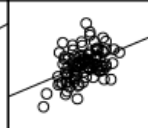
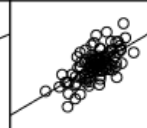
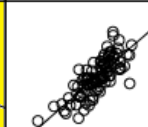
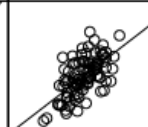
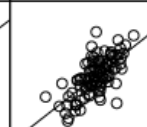
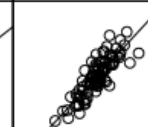
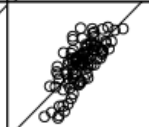
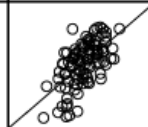
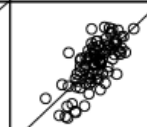
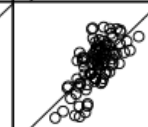
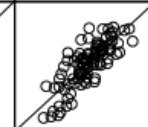
PAS.Cheam		$r = -.528^{**}$ $p = .000$ $N = 96$	$r = -.313^{**}$ $p = .002$ $N = 96$	$r = -.348^{**}$ $p = .001$ $N = 96$	$r = -.519^{**}$ $p = .000$ $N = 96$	$r = -.531^{**}$ $p = .000$ $N = 96$	$r = -.455^{**}$ $p = .000$ $N = 96$	$r = -.388^{**}$ $p = .000$ $N = 96$
BrandyMH			$r = .705^{**}$ $p = .000$ $N = 96$	$r = .639^{**}$ $p = .000$ $N = 96$	$r = .737^{**}$ $p = .000$ $N = 96$	$r = .702^{**}$ $p = .000$ $N = 96$	$r = .785^{**}$ $p = .000$ $N = 96$	$r = .813^{**}$ $p = .000$ $N = 96$
CheamMH				$r = .678^{**}$ $p = .000$ $N = 96$	$r = .598^{**}$ $p = .000$ $N = 96$	$r = .575^{**}$ $p = .000$ $N = 96$	$r = .901^{**}$ $p = .000$ $N = 96$	$r = .728^{**}$ $p = .000$ $N = 96$
CheamSAF					$r = .721^{**}$ $p = .000$ $N = 96$	$r = .436^{**}$ $p = .000$ $N = 96$	$r = .631^{**}$ $p = .000$ $N = 96$	$r = .610^{**}$ $p = .000$ $N = 96$
HurleySAF						$r = .648^{**}$ $p = .000$ $N = 96$	$r = .681^{**}$ $p = .000$ $N = 96$	$r = .713^{**}$ $p = .000$ $N = 96$
JoffreMH							$r = .858^{**}$ $p = .000$ $N = 96$	$r = .664^{**}$ $p = .000$ $N = 96$
Jof& CheMH								$r = .800^{**}$ $p = .000$ $N = 96$
RutherMH								
	PAS.Cheam	BrandyMH	CheamMH	CheamSAF	HurleySAF	JoffreMH	Jof& CheMH	RutherMH

Figure 4.3: Correlation matrices with Pearson's r values for the Mt. Cheam PAS snow data and the seven residual tree-ring chronologies. The yellow highlighted sections of the table display the correlation between PAS and each residual tree-ring chronology individually. A single asterisk (*) indicates significance at the 0.05 level while a double asterisk (**) indicates significance at the 0.01 level.

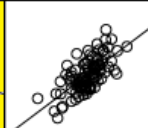
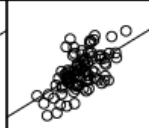
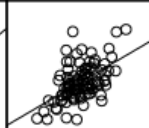
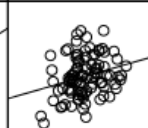
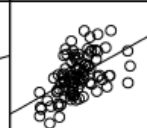
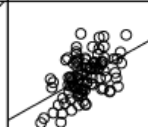
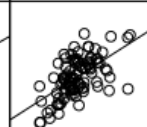
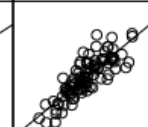
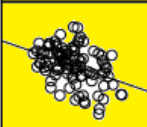
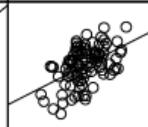
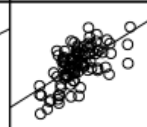
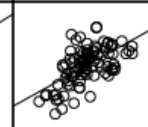
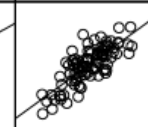
PAS.Cheam		$r = -.548^{**}$ $p = .000$ $N = 96$	$r = -.313^{**}$ $p = .002$ $N = 96$	$r = -.284^{**}$ $p = .005$ $N = 96$	$r = -.529^{**}$ $p = .000$ $N = 96$	$r = -.538^{**}$ $p = .000$ $N = 96$	$r = -.467^{**}$ $p = .000$ $N = 96$	$r = -.396^{**}$ $p = .000$ $N = 96$
BrandyMH			$r = .684^{**}$ $p = .000$ $N = 96$	$r = .540^{**}$ $p = .000$ $N = 96$	$r = .677^{**}$ $p = .000$ $N = 96$	$r = .650^{**}$ $p = .000$ $N = 96$	$r = .761^{**}$ $p = .000$ $N = 96$	$r = .760^{**}$ $p = .000$ $N = 96$
CheamMH				$r = .583^{**}$ $p = .000$ $N = 96$	$r = .539^{**}$ $p = .000$ $N = 96$	$r = .542^{**}$ $p = .000$ $N = 96$	$r = .903^{**}$ $p = .000$ $N = 96$	$r = .731^{**}$ $p = .000$ $N = 96$
CheamSAF					$r = .698^{**}$ $p = .000$ $N = 96$	$r = .260^{*}$ $p = .011$ $N = 96$	$r = .510^{**}$ $p = .000$ $N = 96$	$r = .494^{**}$ $p = .000$ $N = 96$
HurleySAF						$r = .522^{**}$ $p = .000$ $N = 96$	$r = .599^{**}$ $p = .000$ $N = 96$	$r = .627^{**}$ $p = .000$ $N = 96$
JoffreMH							$r = .837^{**}$ $p = .000$ $N = 96$	$r = .603^{**}$ $p = .000$ $N = 96$
Jof& CheMH								$r = .781^{**}$ $p = .000$ $N = 96$
RutherMH								
	PAS.Cheam	BrandyMH	CheamMH	CheamSAF	HurleySAF	JoffreMH	Jof& CheMH	RutherMH

Figure 4.4: Correlation matrices with Pearson's r values for the Mt. Cheam PAS snow data and the seven arstan tree-ring chronologies. The yellow highlighted sections of the table display the correlation between PAS and each arstan tree-ring chronology individually. A single asterisk (*) indicates significance at the 0.05 level while a double asterisk (**) indicates significance at the 0.01 level.

4.2 SWE Reconstruction

There were 26 regression analyses conducted with the SWE data sets. While the majority of regression analyses yielded low coefficient of determination (r^2) values, two had encouraging results. The coefficients of determination and summary of the multiple linear regression models for these two models are summarized in Table 4.1, and the LOO cross-validation statistics are summarized in Table 4.2. Both of the SWE models failed to validate, yielding negative RE values. Because of the negative RE values and the short temporal period for calibration, neither of the SWE models ensued to a reconstruction following the LOO cross-validation (Figure 4.5).

Table 4.1: Overview of the multiple regression analysis for the two best SWE models.

SWE model #1: best overall strength	SWE model #2: best single predictor
<ul style="list-style-type: none"> • ARSTAN chronology model • calibration period = 1949 – 1998 • reconstruction model = 1740 – 1998 • $y = 773.8 - 387.5x_1 - 279.9x_2 + 209.8x_3$ • correlation coefficient (r^2) = 0.374 • dependent variable = LL.April.SWE (y) • independent variables = JoffreMH (x_1); CheamSAF (x_2); and CheamMH (x_3) 	<ul style="list-style-type: none"> • residual chronology model • calibration period = 1949 – 1998 • reconstruction model = 1720 – 1998 • $y = 615.6 - 289.7x$ • correlation coefficient (r^2) = 0.334 • dependent variable = LL.April.SWE (y) • independent variable = BrandyMH (x)

Table 4.2: LOO cross-validation analysis for the two SWE models (described in Table 4.1).

SWE model #1: best overall strength	
<i>Calibration LOO cross-validation statistics:</i>	<i>Validation LOO cross-validation statistics:</i>
<ul style="list-style-type: none"> • $SSE_c = 370947.8$ • $MSE_c = 7418.956$ • $RMSE_c = 86.13336$ • $\Delta RMSE = 16.66377$ 	<ul style="list-style-type: none"> • $SSE_v = 528362.5$ • $MSE_v = 10567.25$ • $RMSE_v = 102.7971$ • RE = - 0.42436
SWE model #2: best single predictor	
<i>Calibration LOO cross-validation statistics:</i>	<i>Validation LOO cross-validation statistics:</i>
<ul style="list-style-type: none"> • $SSE_c = 395369.7$ • $MSE_c = 7907.394$ • $RMSE_c = 88.92353$ • $\Delta RMSE = 4.187771$ 	<ul style="list-style-type: none"> • $SSE_v = 433485.7$ • $MSE_v = 8669.714$ • $RMSE_v = 93.1113$ • RE = - 0.09641

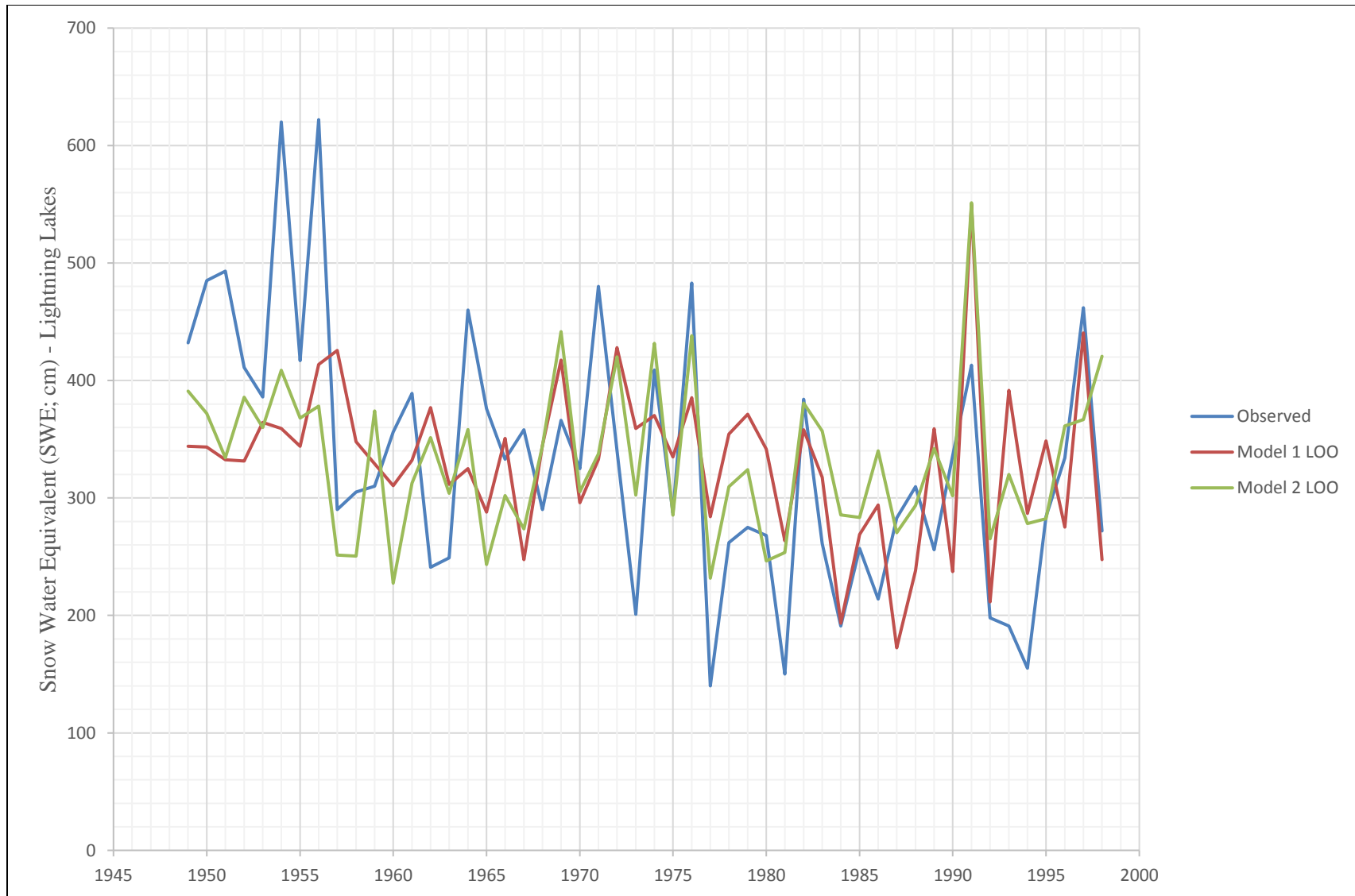


Figure 4.5: Line graph showing the observed SWE compared with results from the LOO cross-validation procedure of both models.

4.3 PAS Reconstruction

PAS was chosen for reconstruction in favour of the SWE datasets because of the longer calibration period (almost twice the length) and larger number of iterations possible. In comparison with the 26 SWE trials, 180 PAS multiple linear regression analyses were considered. The majority yielded low coefficients of determination (r^2 values); however, there were two models that had at least enough of a correlation to investigate. Similar to the material presented in Tables 4.1 and 4.2 for the SWE models; Tables 4.3 and 4.4 below outline the linear regression models, correlations, and statistics related to the LOO cross-validation procedure.

Table 4.3: Overview of the multiple regression analysis for the two best PAS models.

PAS model #1: best overall strength	PAS model #2: 95-yr longer reconstruction
<ul style="list-style-type: none"> • ARSTAN chronology model • calibration period = 1902 – 1997 • reconstruction model = 1835 – 1997 • $y = 2060.6 - 275.0x_1 - 516.5x_2 - 399.3x_3$ • correlation coefficient (r^2) = 0.391 • dependent variable = PAS.Cheam (y) • independent variables = BrandyMH (x_1); JoffreMH (x_2); and HurleySAF (x_3) 	<ul style="list-style-type: none"> • ARSTAN chronology model • calibration period = 1902 – 1997 • reconstruction model = 1740 – 1997 • $y = 1918.4 - 476.1x_1 - 582.2x_2$ • correlation coefficient (r^2) = 0.358 • dependent variable = PAS.Cheam (y) • independent variable = BrandyMH (x_1); and JoffreMH (x_2)

Table 4.4: LOO cross-validation analysis for the two PAS models (described in Table 4.3).

PAS model #1: best overall strength	
<i>Calibration LOO cross-validation statistics:</i>	<i>Validation LOO cross-validation statistics:</i>
<ul style="list-style-type: none"> • $SSE_c = 4650289$ • $MSE_c = 48440.5$ • $RMSE_c = 220.092$ 	<ul style="list-style-type: none"> • $SSE_v = 5363851$ • $MSE_v = 55873.5$ • $RMSE_v = 236.376$
• $\Delta RMSE = 16.2836$	• RE = - 0.15344
PAS model #2: 95-yr longer reconstruction	
<i>Calibration LOO cross-validation statistics:</i>	<i>Validation LOO cross-validation statistics:</i>
<ul style="list-style-type: none"> • $SSE_c = 4900414$ • $MSE_c = 51046.0$ • $RMSE_c = 225.934$ 	<ul style="list-style-type: none"> • $SSE_v = 5068118$ • $MSE_v = 52792.9$ • $RMSE_v = 229.767$
• $\Delta RMSE = 3.83348$	• RE = - 0.03422

As noted, the LOO cross validation procedure carried out on the four models (two SWE and two PAS models) produced negative RE values, which suggests that this analysis failed to find any model that had robust predictive reconstruction skill. Despite this outcome, the second PAS model visually appears to be fairly representative of the observed dataset (Figure 4.6). It yielded consistent calibration and validation results, and had an RE value close to zero. Given these findings and relationships, it seemed appropriate, even in light of the failed statistical results of the LOO cross-validation procedure, to undertake further analyses.

Using the multiple linear regression model for PAS model #2 ($y = 1918.4 - 476.1x_1 - 582.2x_2$; found in Table 4.3), and the mountain hemlock tree-ring chronologies from Brandywine Creek and Joffre, a PAS reconstruction back to 1740 AD was completed. Figures 4.7 through 4.10 illustrate: the reconstruction with confidence intervals (Figure 4.7), the reconstruction represented relative to the mean observed PAS value (Figure 4.8), the reconstruction overlain with a five-year running mean (Figure 4.9), and the reconstruction overlain with an eleven-year running mean (Figure 4.10).

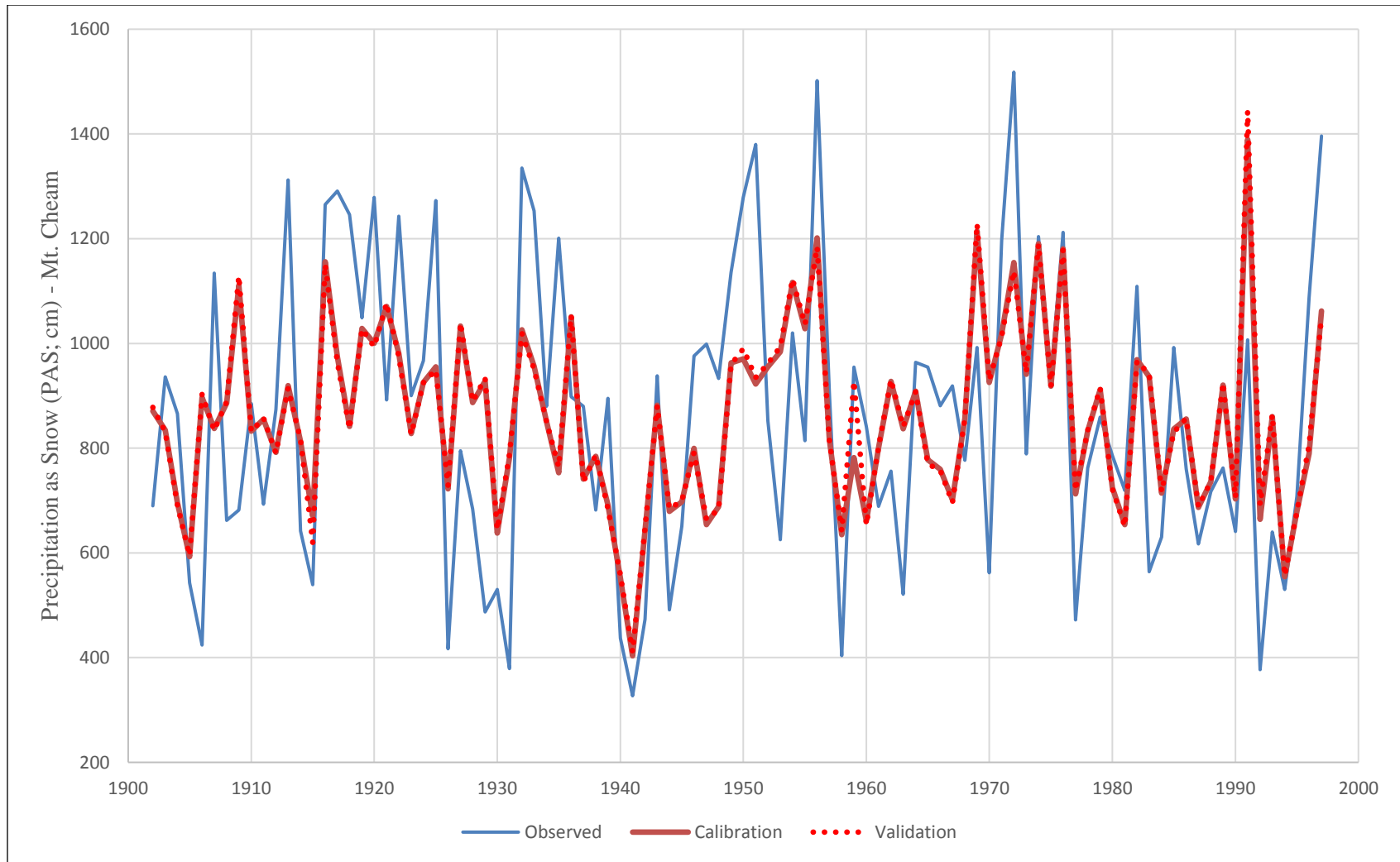


Figure 4.6: Line graph depicting the closeness of the calibration and validation datasets for the LOO cross-validation of PAS model #2. The general consistency between the calibration and validation lines, in conjunction with the close to positive RE value (-0.03422), were the two dominant reasons for pursuing the PAS model #2 in the reconstruction stage of this research project; even with the acceptance that a negative RE value should be considered a failed reconstruction because it shows no statistical robustness.

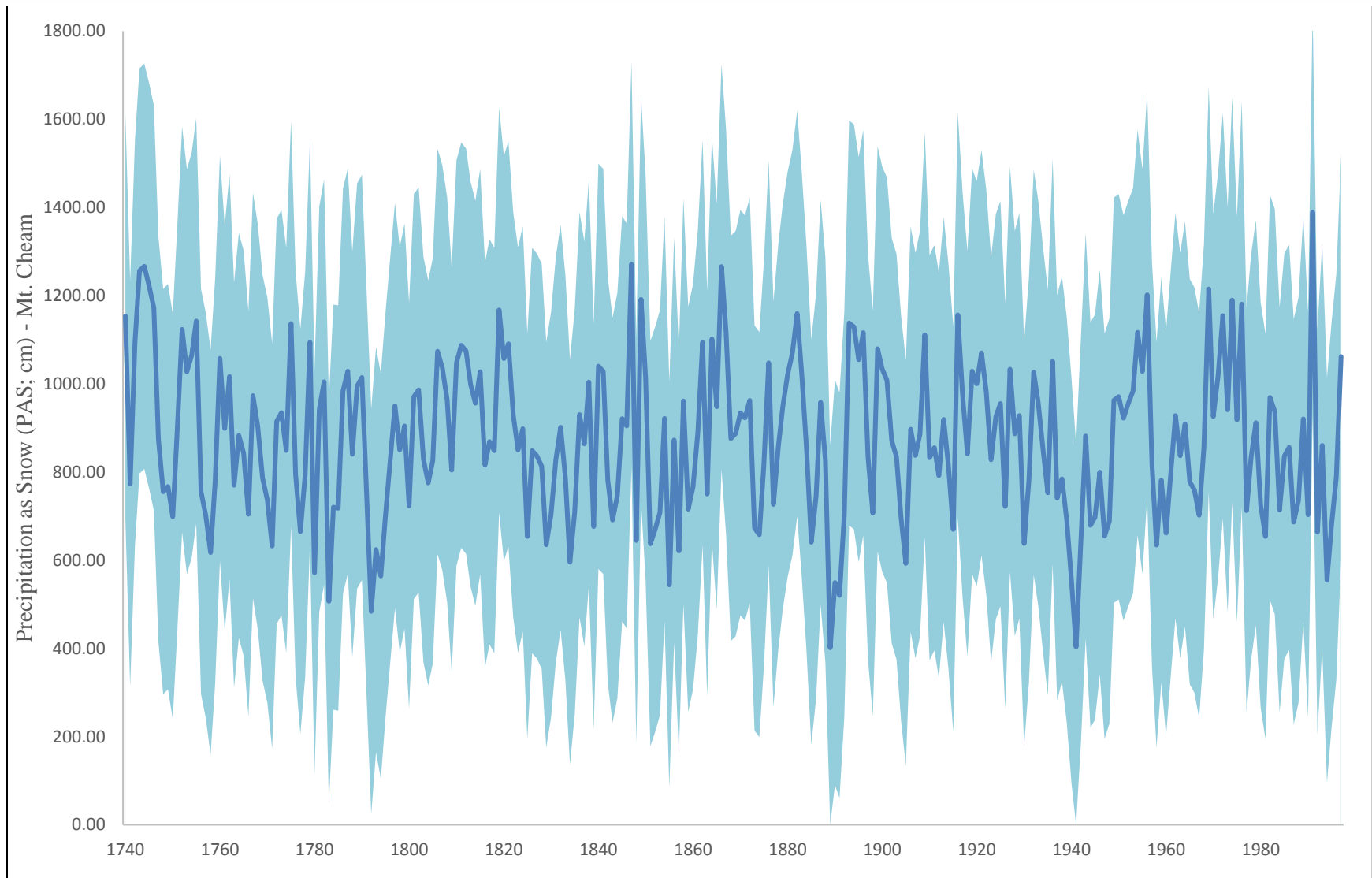


Figure 4.7: PAS reconstruction (dark line) over top of the confidence intervals associated with the reconstruction. The confidence intervals were calculated based on RMSE values, so the fairly large ranges are expected considering the negative RE values.

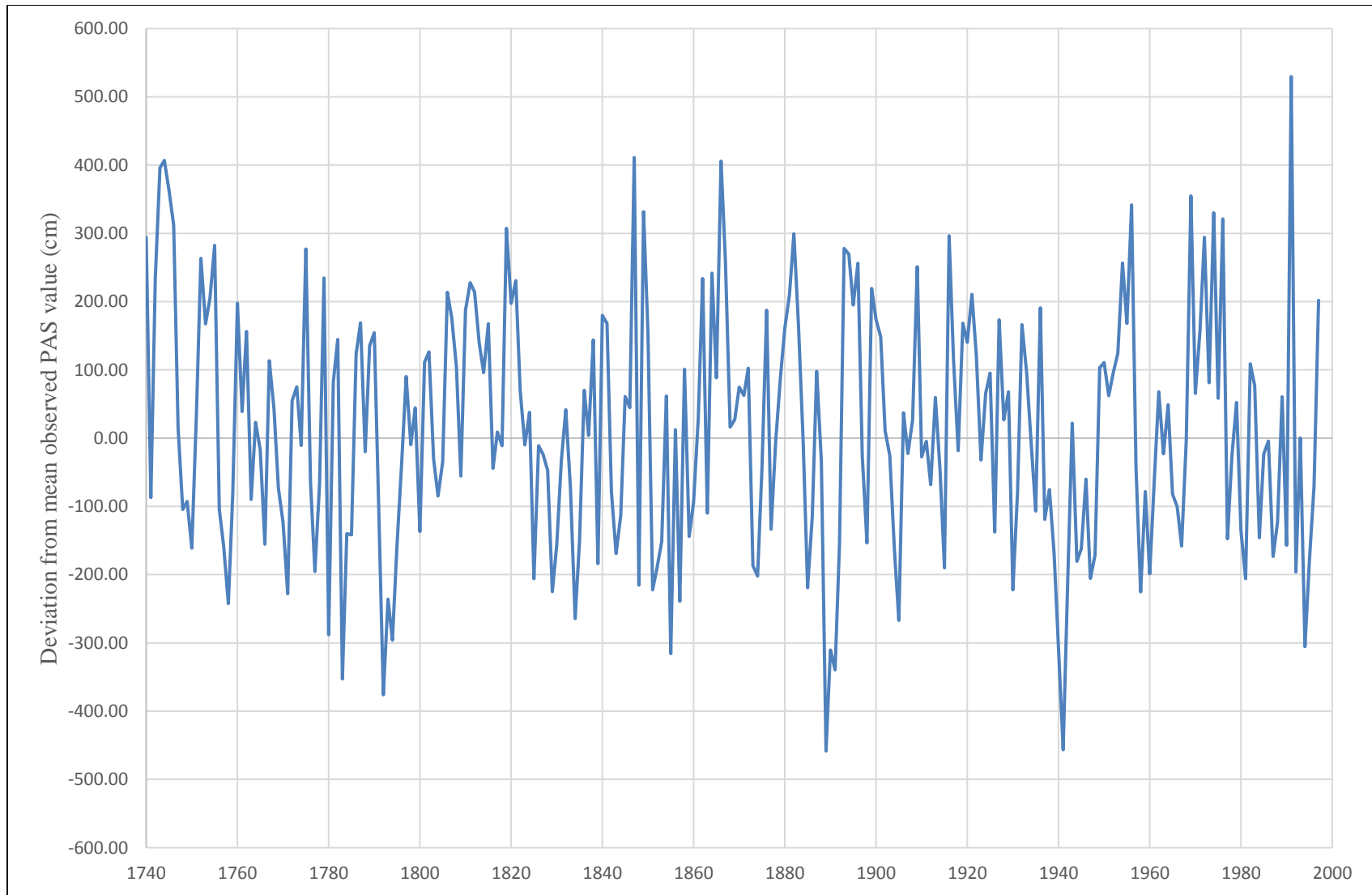


Figure 4.8: PAS reconstruction represented as a deviation from the mean annual observed PAS value. Years below the zero-line had lower than average PAS values, and years above the zero-line had above average PAS values.

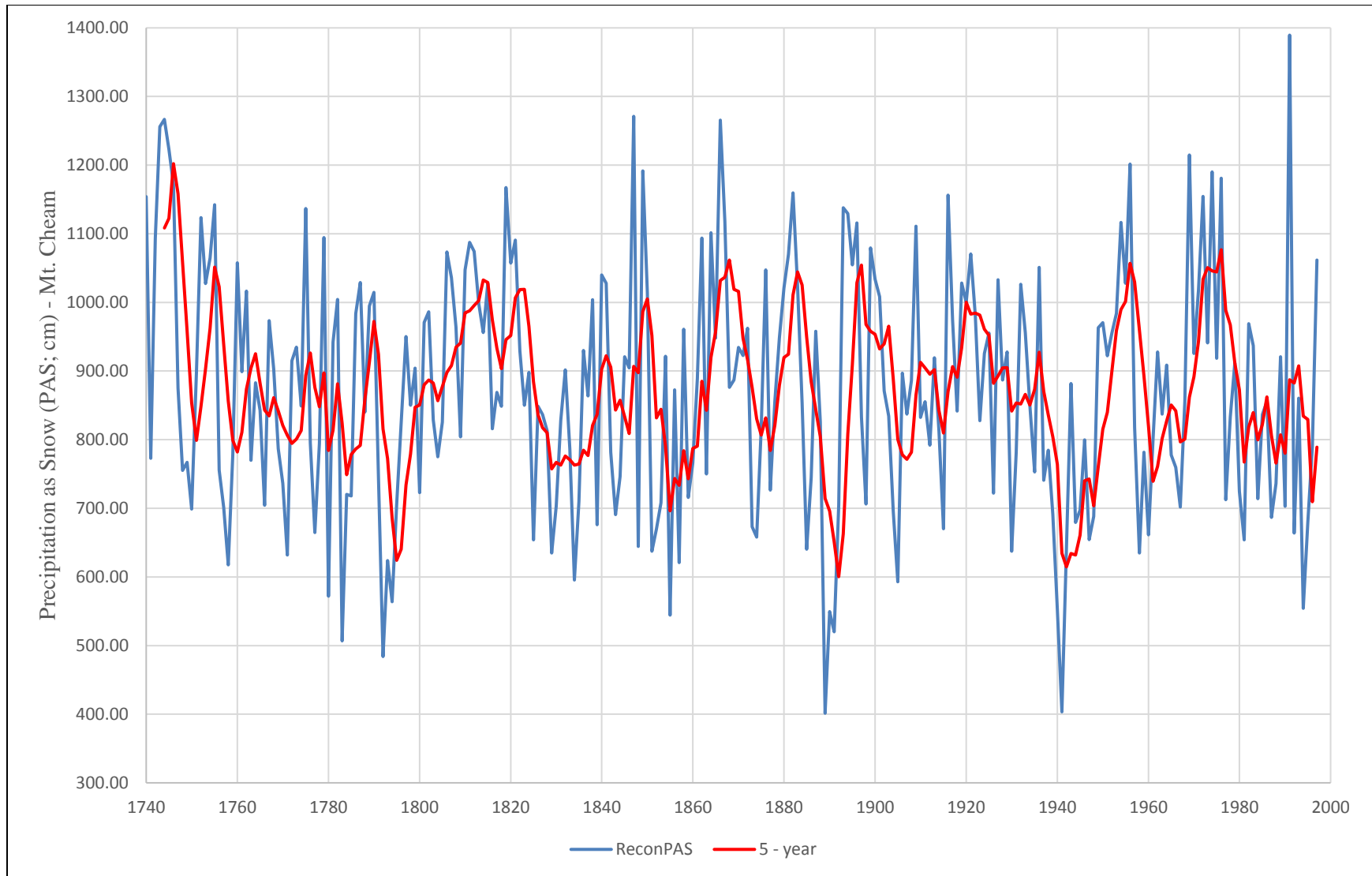


Figure 4.9: PAS reconstruction (blue line) with the five-year running mean (red line) overlain to highlight possible cyclical patterns.

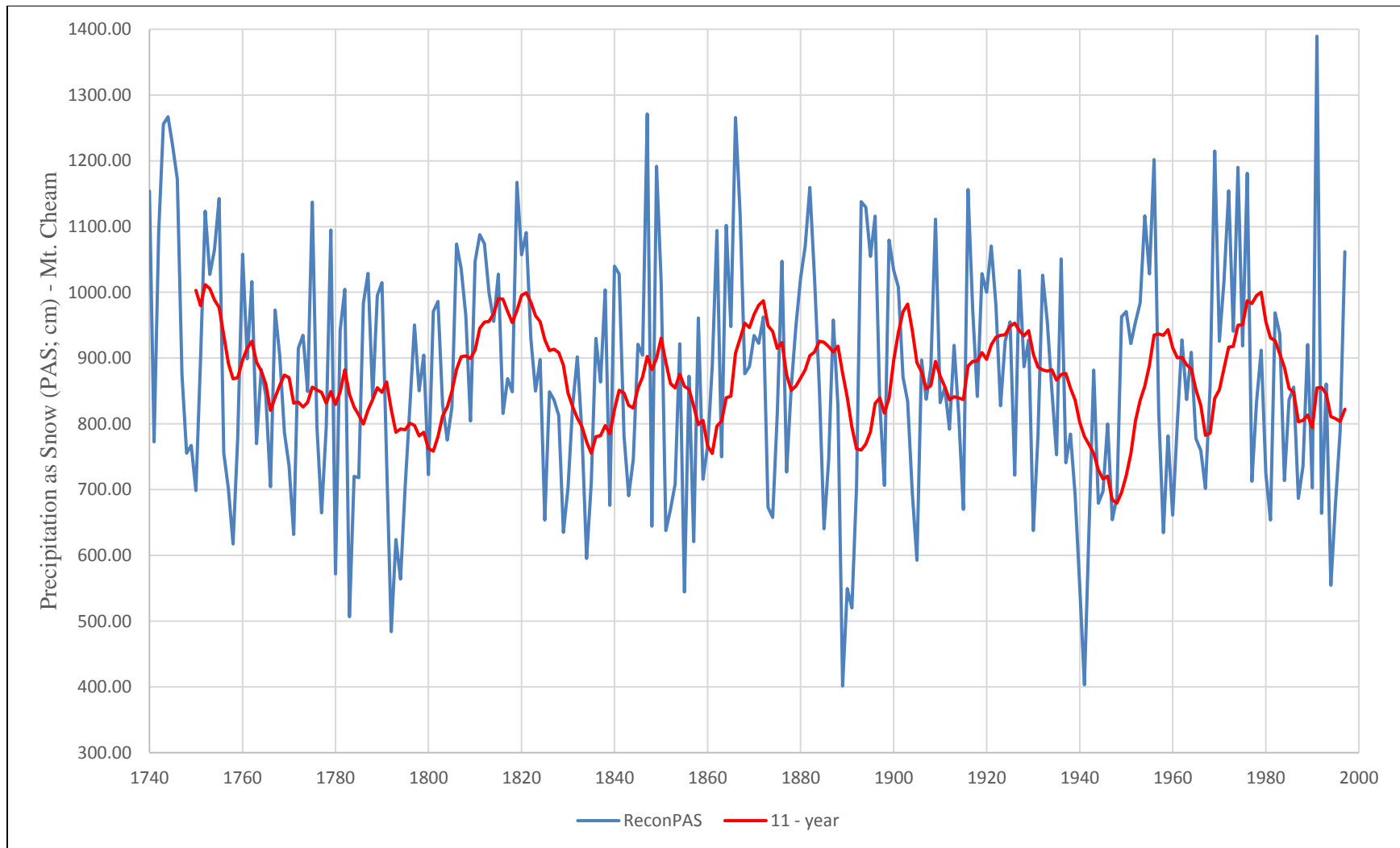


Figure 4.10: PAS reconstruction (blue line) with the eleven-year running mean (red line) overlain. Longer-scale cyclical patterns can be seen in this running mean, although identifying the underlying causes of lower-frequency cyclicity is difficult.

CHAPTER FIVE: DISCUSSION

5.1 Interpretation

Two snow variables were examined as part of this research, snow water equivalent (SWE) and precipitation as snow (PAS). SWE had the advantage of being determined from observed data that have been collected yearly via field staff, but was constrained by a relatively short temporal period (50 years). PAS had the advantage of having almost double the temporal duration as SWE, but is a model-derived calculated variable that may or may not accurately reflect the actual (instrument observed) snowpack environment. In the end, all of the SWE and PAS models failed to produce successful validated reconstruction models. Nonetheless, the findings do provide useful insights and these are discussed below.

Most previous snowpack reconstructions presented in the literature were developed by using SWE datasets for calibration, so it was logical to start this study by examining SWE data and attempting to perform a SWE reconstruction. Although the aforementioned short temporal duration of SWE data impacted the linear regression capabilities of the models, it seems likely that the SWE models failed due to a lack of regionalized data. Snowfall is spatially variable, as discussed later in Section 5.3, and regionalization can assist in transforming the data into something that behaves more robustly with regression analysis. A snow course is completed by taking a standard of 20 point measurements along a linear line and the locations are selected to be as representative of the regional snow as possible. The measurement locations are repeated every year which provides inter-annual consistency. Nonetheless, in regions with multiple annual snow courses, a combined regionalized value can be calculated using available snow course data which may be more representative. This can be accomplished through methods such as principle component analysis or partial least square regression (i.e., Timilsena & Piechota, 2008).

Following failure of the SWE models, the winter summed PAS data was examined. From the onset it was recognized that the usefulness of PAS data is constrained by two things. First, PAS is a model-derived variable. The PAS used in this research came from the program ClimateWNA, which extracts climate parameters over half square kilometre areas (Wang et al., 2012). Using a model-derived variable as if it was an observed variable can be appropriate; however, caution must be given to ensure that the variable is actually representative of what it should be. Second, PAS does not explicitly represent the snowpack depth, while SWE does. PAS is a measure of the amount of snow input (precipitation falling as snow) into a snowpack, but it does not take into account any snow redistribution (which often averages over a large area) or any snow loss from melting or sublimation. By summing the total winter PAS in this study, the total amount of snow input was derived; however, this value is inflated in comparison to what an observed snowpack value is because it does not account for any loss of snow. A correction for this was considered, but it was deemed excessive for this project due to the exploratory nature of this research and was instead listed later as a recommendation for future research.

5.2 Historical Trends in the Snowpack History

An examination of the PAS reconstruction with running means (Figures 4.9 and 4.10) illustrates the historic annual variability of PAS in this region. There are two key observations. First, the earliest portion of the PAS reconstruction displays a higher degree of annual variability. There are two interpretations for the increased annual variability; either that the eighteenth century had a greater degree of annual climatic fluctuations, perhaps due to an increase in strength of some of the aforementioned cyclical climatic factors (i.e., PDO), or that the inflated

variance in the early part of a reconstruction is likely due to a drop in sample size, which is a common statistical limitation of hindcasting.

The second observation is that the reconstruction period emphasized a different periodicity than the calibration period. The calibration period suggests a PAS cycle with an eleven years' period, whereas the reconstruction period illustrates a periodicity that is roughly double in duration. This is problematic because the calibration period is the only part of a reconstruction that can be cross-examined with the climate data being reconstructed. Although this issue is most likely related to the lack of statistical robustness, there is a small possibility that the duration and strengths of the cyclical climatic factors were different in the past, or that the degree to which the impacts from them overlapped was stronger during the reconstruction period; this is, however, speculation derived from interpreting this one reconstruction.

Low snowpack years in PNA are believed associated with either positive PNA circulation patterns, such as the PDO or La Nina phases of the ENSO circulation patterns (Woodhouse, 2003). From visual examination of the PAS reconstructions (Figures 4.7 – 4.10), both of these cyclic climate patterns appear to be present. The approximately five-year (three- to seven-year) ENSO patterns are more pronounced in the calibration period as opposed to the reconstruction period; whereas the approximately decadal (about 11-year) PDO patterns are more pronounced in the reconstruction period as opposed to the calibration period. This observation limits any interpretation about the long-term snowpack history because the reconstruction period failed to emphasize the same dominant pattern.

Pederson et al. (2011) suggest there were only two periods of sustained low snowpacks (20-30 years) in the last 800 years that are comparable to the low snowpack periods observed during the early- and late- twentieth century. They indicate that these periods were the result of

PDO and ENSO affecting the temperature in the latter half of the critical snow accumulation period starting in February each year (Pederson et al., 2011). The sustained low snowpack period mentioned in the early-twentieth century (1895-1915) appears in the reconstruction produced by this study, along with another sustained low snowpack period in the nineteenth century (1825-1855) that was not mentioned in the literature reviewed.

5.3 Reconstruction Comparisons

A comparison between the PAS reconstruction completed as part of this research and two SWE reconstructions completed by Starheim et al. (2013) are depicted below in Figures 5.1 and 5.2. The blue lines show the PAS reconstruction from this study, and the red lines show the SWE reconstruction of Tatlayoko (Figure 5.1) and Mt. Cronin (Figure 5.2) (Starheim et al., 2013). From a visual analysis of these two figures, it is evident that there are minimal relationships between my PAS reconstruction and the Tatlayoko and Mt. Cronin SWE reconstructions completed previously by Starheim et al. (2013). Specifically, although some extreme (low and high) snow years correspond between the PAS and SWE reconstructions, many of the specific years have opposite snow extremes (low in one and high in the other, and vice versa) (Figures 5.1 and 5.2). As Tatlayoko and Mt. Cronin are both located in the BC Coast Mountains, it was anticipated that there would be more similarities between these SWE reconstructions and the PAS reconstruction completed as part of this research; however, the lack of relationships are likely due in part to the aforementioned lack of statistical success of the PAS reconstruction within this research study (Starheim et al., 2013).

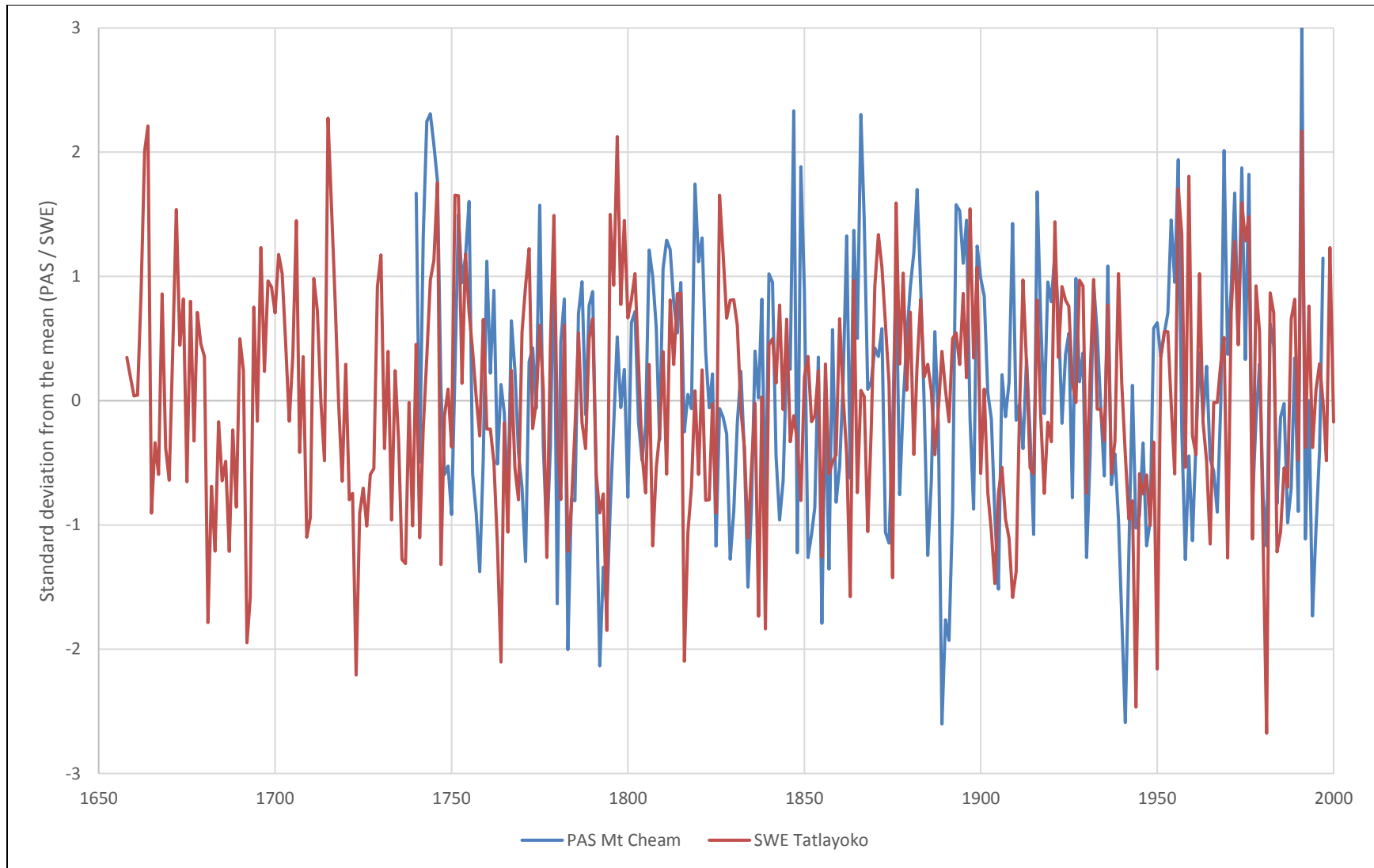


Figure 5.1: Line graph comparing the PAS reconstruction from this research study (blue line) to the Tatlayoko SWE reconstruction completed by Starheim et al. (2013) (red line); displayed as the annual standard deviation from the mean SWE and PAS values.

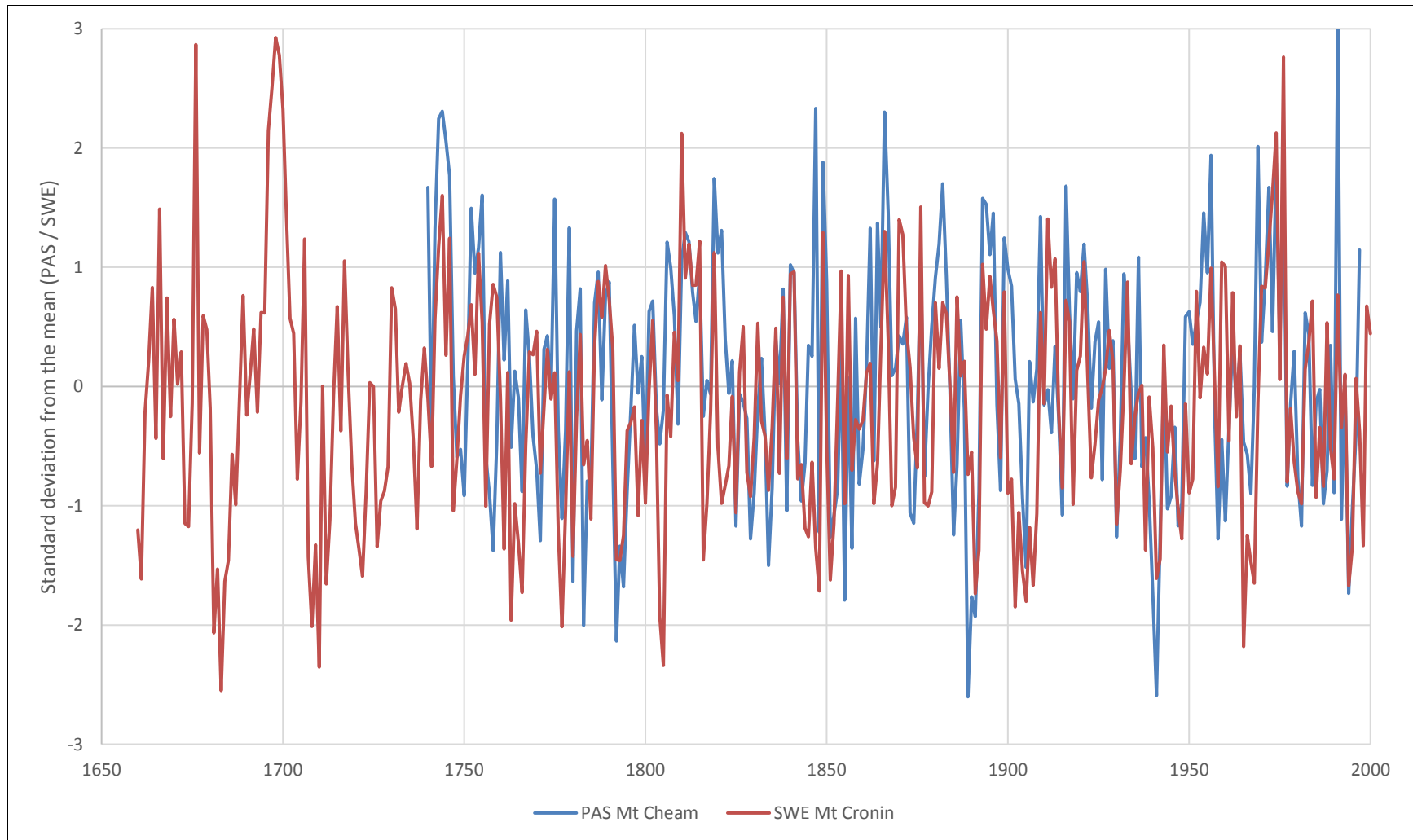


Figure 5.2: Line graph comparing the PAS reconstruction from this research study (blue line) to the Mt. Cronin SWE reconstruction completed by Starheim et al. (2013) (red line); displayed as the annual standard deviation from the mean SWE and PAS values.

5.4 Difficulties Associated with a Snowpack Reconstruction

It should be noted that any snowpack, regardless of location, will exhibit a large degree of spatial (expressed horizontally in a snowpack) and temporal variability (expressed vertically in a snowpack). Spatial variability is inherent in all stages of snowpack development, from depositional differences, such as the presence of canopy cover, through redistribution and transport, where snow is typically redistributed into a less uniform condition, to snowmelt, where snow in cooler and more shaded areas remains longest. Snow typically deposits in horizontal layers with each layer representing a snowfall event, although these layers can often be affected by snow redistribution and snowmelt. Over the period of snowpack development, many different snowfall events build the horizontal layers and a vertical time stratum is created. Similar to the spatial variability, the vertical time stratum is bound by temporal variability based on both the same factors as the spatial variability, and factors related to changing climates over the snowpack development period. When combined, the spatial and temporal variability yields a large degree of overall variability in regards to the depth of snow present at any one point.

Snow metamorphism (temperature gradient and equi-temperature metamorphism) further increases the difficulties of creating a snowpack reconstruction above and beyond large spatial and temporal variability. This ranges from simple snowpack alteration from compression of new snow falling onto older snow, to more complex morphology such as the presence of snowmelt channels or the creation of depth hoar. It is sufficient to say that a snowpack is far from uniform.

In addition to the inherent variability of a snowpack, there are a number of factors that could have yielded the negative results observed in this research, and are discussed in detail throughout the remainder of this section. There is a short calibration period, particularly with the SWE dataset. A short calibration period is an important issue because this is the timeframe that a

dendroclimatological reconstruction has to align with the observed data that is available. The longer the calibration period, the more likely the reconstructed model is aligned and actually representative of the data it is attempting to reconstruct. Supplementary to the short calibration period itself, the specific interval of the calibration period where the instrumental and tree-ring data overlaps can influence the reconstruction and contribute to the negative results observed. Specifically, if the interval of overlap captures a certain climatic event (such as a PDO switch) that increases the “noise” within the calibration period, then the models may have suffered because of a lowered signal-to-noise ratio within the climate-growth relationship.

In discussing the signal-to-noise ratio, a probable cause of the observed negative results is a weak underlying climate signal. In order to have a strong signal, the tree-ring sample sites should be located at extreme limiting-point of their distribution. For the MH trees examined in this study (energy-limited and negatively correlated with snow depth), the sampling sites should have been located at the high elevations closest to the top of the subalpine zone (near the elevation shift to the alpine zone). Furthermore, the signal-to-noise ratio may have been reduced due to stand-level disturbances including: blow down, insect infestations and fire; or even micro-scale disturbances such as winter limb breakage. These are just some of the many factors that may have reduced the signal-to-noise ratio and contributed to the negative results observed.

Regionalization might also help to enhance the climate signal (i.e., increase the signal to noise ratio); although this should be done with some degree of caution to avoid data “fishing”. Regionalizing the snow data has been previously discussed, but it should be noted that the tree-ring chronologies could also be regionalized. In the same manner as regionalized snow data, regionalized tree-ring chronologies may be more representative of the area as a whole. Of

particular interest for future research, regionalizing both data under the same parameters may result in stronger resultant climate-growth relationships.

Lastly, as noted earlier in Chapter 2, some MH in PNA began to demonstrate climate-growth divergence behaviour beginning after 2000 (Coulthard 2015; Marcinkowski et al., 2015). A divergence between climate data (snow) and tree response (tree-ring chronologies) is a crucial issue because an important assumption for dendroclimatological reconstructions is time stability of the tree ring-climate relationship. The reported divergence is an issue in recent years (starting in 2000); so this was specifically avoided in this research by cutting off all data at the end of 1998. Nonetheless, the divergence (lack of time stability) is important to keep in mind, especially for any future research in the Pacific Northwest of Canada and the USA.

CHAPTER SIX: CONCLUSION

6.1 Introduction

Over the last century there has been an overall snowpack decline in Pacific North America (PNA) with numerous implications for water availability during summer months. Snowpacks are impacted by both natural fluctuations and by climate change, but isolating these impacts is the key challenge to recent large-scale snowpack research. Two major limitations are present with analysis of snowpacks for climatic research. First, snowpacks have a high degree of spatiotemporal variability. Second, instrumental snow data is of limited temporal duration. Snow water equivalent (SWE) is a measured snow variable that typically is limited to the last half century; while precipitation as snow (PAS) is a modelled variable that provides insight into a snowpack that can temporally span a full century. Even a full century can be insufficient for climatic research. To extend the snow record further than is available with data, researchers often use climatic proxies. One such climatic proxy is the use of tree-ring chronologies for dendroclimatological analysis.

6.2 Thesis Summary

The research presented in the thesis intended to develop a proxy dendroclimatic record of historic snowpack characteristics in the southern British Columbia (BC) Coast Mountains. Seven representative tree-ring chronologies from five study sites were obtained, and the chronologies were detrended and standardized to serve as snow data proxies. SWE data was obtained from all available snow courses in this region and PAS data was obtained as point data at each of the five study sites. After examination of tree ring-snow correlations, only the SWE data from Lightning Lakes and PAS data from Mt. Cheam (near Lightning Lakes) were considered. From a statistical

perspective, the PAS datasets were deemed better because of higher correlation values; however, the SWE datasets are the logical choice as they are more representative of the annual snowpack.

Over 200 model-iteration trials were performed to reveal any statistical skill of the tree-ring chronologies for predicting snow. The majority of all of these trials were discarded due to extremely low coefficient of determination (r^2) values. Only the two best SWE models and PAS models were retained for RE analyses and validation. Unfortunately, all four models failed RE validation. Failure of the SWE models was believed to be due in part to the short calibration period (under fifty years), with the proxy SWE data unable to reconstruct the observed SWE data. In contrast, the PAS models did not pass the validation procedure, but there was reasonable visual relationship between the modelled and observed PAS data. Given this, the two PAS models extrapolated from the PAS data were considered. PAS model #2 was deemed superior to PAS model #1 because model #2 had an RE value that was almost positive and had a 95-year longer reconstruction period, and as such was used for the PAS reconstruction.

Two interpretations of historic snowpack patterns were presented based on the PAS reconstruction. One interpretation was that the reconstruction period was emphasizing a different snow patterns than in the calibration period. Another interpretation was that there was increased annual variability in the earlier half of the reconstruction. Numerous difficulties exist around performing snow reconstructions, including the following three examples. First, snowpacks have a high degree of spatiotemporal variability. Second, snow data is often constrained by a short calibration period. Third, a weak climate signal due to site location/elevation, stand disturbances or divergence may reduce the signal to noise ratio and produce less statistically robust climate-growth relationships with which to produce a reconstruction with. It is anticipated that these difficulties will provide insight for future work on snow reconstructions.

6.3 Conclusion

The aim of this thesis was to complete a dendrochronological snow reconstruction using available tree-ring chronologies and snow data from the southern BC Coast Mountains. Tree-ring chronologies for both mountain hemlock and subalpine fir trees and snow datasets derived from SWE and PAS were used. Correlation analysis and subsequent numerous linear regression models were attempted to obtain the most promising model and from these, two SWE and two PAS models were pursued. These models had coefficient of determination (r^2) values between 0.334 and 0.391, and all four of them failed to validate during the leave-one-out cross validation method. This project did not succeed in the goal of producing a statistically validated PAS reconstruction. A single reconstruction was carried out, however, to address the research objectives and act as a benchmark for further research.

6.4 Recommendations for Future Research

Although the research did not result in a statistically validated PAS reconstruction, it did enable recommendations for future research. The number of tree-ring chronologies used in this study would likely have been adequate, if the climate-growth relationship had been stronger; however, increasing the quantity of chronologies could improve the probability of finding stronger climate-growth relationships between variables. As such, the first recommendation for future research, particularly further work in the same region, is to assemble more tree-ring chronologies from the southern Coast Mountains.

A second recommendation is to consider regionalizing the snow data. As discussed, snowpacks have a large degree of spatiotemporal variability. Most successful snow reconstructions have employed some form of data regionalization, such as principle component

analysis or partial least square regression. Regionalization of the snow data could be beneficial because a combination of snow courses or point PAS datasets could remove any small site-specific noise that is not common to the region as a whole. This study specifically chose to run a dendrochronological PAS reconstruction without first performing a regionalization of the snow data; however, regionalization may have produced better results.

One of the problems that arose specifically with using PAS snow data, is the unrealistic nature of summing all of the winter monthly PAS information and not taking snow loss factors (melt, sublimation, transport, etc.) into consideration. To correct for this difficulty, a researcher could employ a simple degree day snowmelt model to determine the amount of snow loss, and thus develop a more accurate snow parameter with PAS. This degree day snowmelt model correction is the third recommendation for future research.

REFERENCES

- Anderson, S., Moser, C.L., Tootle, G.A., Grissino-Mayer, H.D., Timilsena, J., & Piechota, T. (2012). Snowpack reconstructions incorporating climate in the upper Green River Basin (Wyoming). *Tree-Ring Research*, 68, 105-114.
- Antos, J.A., & Parish, R. (2002). Dynamics of an old-growth, fire-initiated, subalpine forest in southern interior British Columbia: tree size, age, and spatial structure. *Canadian Journal of Forest Research*, 32, 1935-1946. doi:10.1139/X02-116
- Barnett, T.P., Adam, J.C., & Lettenmaier, D.P. (2005). Potential impacts of a warming climate on water availability in snow-dominated regions. *Nature Reviews*, 438, 303-309. doi:10.1038/nature04141
- Belmecheri, S., Babst, F., Wahl, E.R., Stahle, D.W., & Trouet, V. (2015). Multi-century evaluation of Sierra Nevada snowpack. *Nature Climate Change*, 2 pages.
- British Columbia Ministry of Forests. (1997). *The Ecology of the Mountain Hemlock Zone*. Retrieved from: <https://www.for.gov.bc.ca/hfd/pubs/docs/bro/bro51.pdf>
- Chapman, A. (2007) Trend in April 1st snow water equivalent at long-term British Columbia snow courses, in relation to ENSO, PDO, and Climate Warming. *BC Ministry of Environment*, report from the River Forecast Centre, 7 pages.
- Cleaveland, M.K. (2000). A 963-year reconstruction of summer (JJA) streamflow in the White River, Arkansas, USA, from tree-rings. *The Holocene*, 10, 33-41.
- Coulthard, B. (2015). Multi-century records of snow water equivalent and streamflow drought from energy-limited tree rings in south coastal British Columbia. Unpublished Ph.D. thesis, University of Victoria, Victoria, B.C., Canada.
- Coulthard, B., & Smith, D.J. (2015). A 477-year dendrohydrological assessment of drought severity for Tsable River, Vancouver Island, British Columbia, Canada. *Hydrological Processes*, 30, 1676-1690. doi:10.1002/hyp.10726
- Coulthard, B., Smith, D.J., & Meko, D.M. (2016). Is worst-case scenario streamflow drought underestimated in British Columbia? A multi-century perspective for the south coast, derived from tree-rings. *Journal of Hydrology*, 534, 205-218.
- D'Arrigo, R.D., Kaufmann, R.K., Davi, N., Jacoby, G.C., Laskowski, C., Myneni, R.B., & Cheubini, P. (2004). Thresholds for warming-induced growth decline at elevational tree line in the Yukon Territory, Canada. *Global Biogeochemical Cycles*, 18, 7 pages. doi:10.1029/2004GB002249

- Flower, A., & Smith, D.J. (2011). A dendroclimatic reconstruction of June-July mean temperature in the Northern Canadian Rocky Mountains. *Dendrochronologia*, 29, 55-63. doi:10.1016/j.dendro.2010.10.001
- Fritts, H.C., Guiot, J., & Gordon, G.A. (1990). Verification. In *Methods of Dendrochronology: Applications in the Environmental Sciences*, Cook ER, Kairūkštis L (eds), 178-184.
- Gedalof, Z., & Smith, D.J. (2001). Interdecadal climate variability and regime-scale shifts in Pacific North America. *Geophysical Research Letters*, 28, 1515-1518.
- Graumlich, L.J., & Brubaker, L.B. (1986). Reconstruction of annual temperature (1590-1979) for Longmire, Washington, derived from tree rings. *Quaternary Research*, 25, 223-234.
- Grier, C.C. (1988). Foliage loss due to snow, wind, and winter drying damage: Its effects on leaf biomass of some western conifer forests. *Canadian Journal of Forest Research*, 18, 1097-1102.
- Hart, S.J., Smith, D.J., & Clague, J.J. (2010). A multi-species dendroclimatic reconstruction of Chilko River streamflow, British Columbia, Canada. *Hydrological Processes*, 24, 2752-2761. doi:10.1002/hyp.7674
- Klinka, K., Pojar, J., & Meidinger, D.V. (1991). Revision of biogeoclimatic units of coastal British Columbia. *Northwest Science*, 65, 32-47.
- Larocque, S.J., & Smith, D.J. (2005). A dendroclimatological reconstruction of climate since AD 1700 in the Mt. Waddington area, British Columbia Coast Mountains, Canada. *Dendrochronologia*, 22, 93-106. doi:10.1016/j.dendro.2005.02.003
- Laroque, C.P., Lewis, D.H., & Smith, D.J. (2000/01). Treeline dynamics on Southern Vancouver Island, British Columbia. *Western Geography*, 10/11, 43-63.
- Laroque, C.P., & Smith, D.J. (2005). Predicted short-term radial-growth changes of trees based on past climate on Vancouver Island, British Columbia. *Dendrochronologia*, 22, 163-168. doi:10.1016/j.dendro.2005.04.003
- Laroque, C.P., & Smith, D.J. (1999). Tree-ring analysis of yellow-cedar on Vancouver Island, British Columbia. *Canadian Journal of Forest Research*, 29, 115-123.
- Littell, J.S., Peterson, D.L., & Tjoelker, M. (2008). Douglas-fir growth in mountain ecosystems: Water limits tree growth from stand to region. *Ecological Monographs*, 78, 349-368.
- Loaiciga, H.A., Haston, L., & Michaelsen, J. (1993). Dendrohydrology and long-term hydrologic phenomena. *Reviews of Geophysics*, 31, 151-171.

- Lutz, E.R., Hamlet, A.F., & Littell, J.S. (2012). Paleoreconstruction of cool season precipitation and warm season streamflow in the Pacific Northwest with applications to climate change assessments. *Water Resources Research*, 48, 16 pages. doi:10.1029/2011WR010687
- Mantua, N.J., & Hare, S.R. (2002). The Pacific Decadal Oscillation. *Journal of Oceanography*, 58, 35-44.
- Marcinkowski, K., Peterson, D.L., & Ettl, G.J. (2015). Nonstationary temporal response of mountain hemlock growth to climatic variability in the North Cascade Range, Washington, USA. *Canadian Journal of Forest Research*, 45, 676-688.
- Masiokas, M.H., Villalba, R., Christie, D.A., Betman, E., Luckman, B.H., Le Quesne, C., Prieto, M.R., & Mauget, S. (2012). Snowpack variations since AD 1150 in the Andes of Chile and Argentina (30°-37°S) inferred from rainfall, tree-ring and documentary records. *Journal of Geophysical Research*, 117, 11 pages. doi:10.1039/2011JD016748
- McCabe, G.J., & Clark, M.P. (2005). Trends and variability in snowmelt runoff in the Western United States. *Journal of Hydrometeorology*, 6, 476-482.
- McKenzie, D., Hessel, A.E., & Peterson, D.L. (2001). Recent growth of conifer species of western North America: Assessing spatial patterns of radial growth trends. *Canadian Journal of Forest Research*, 31, 526-538. doi:10.1139/cjfr-31-3-526
- Meko, D.M., Therrell, M.D., Baisan, C.H., & Hughes, M.K. (2001). Sacramento River flow reconstructed to A.D. 869 from tree-rings. *Journal of the American Water Resources Association*, 37, 1029-1038.
- Moore, R.D., & McKendry, I.G. (1996). Spring snowpack anomaly patterns and winter climatic variability, British Columbia, Canada. *Water Resources Research*, 32, 623-632.
- Mote, P.W. (2003a). Trends in temperature and precipitation in the Pacific Northwest during the twentieth century. *Northwest Science*, 77, 271-282.
- Mote, P.W. (2003b) Trends in snow water equivalent in the Pacific Northwest and their climatic causes. *Geophysical Research Letters*, 30, 4 pages. doi:10.1029/2003GL017258
- Mote, P.W., Hamlet, A.F., Clark, M.P., & Lettenmaier, D.P. (2005). Declining mountain snowpack in western North America. *Bulletin of the American Meteorological Society*, January, 39-49. doi:10.1175/BAMS-86-1-39
- Nelson, T.A., Laroque, C.P., & Smith, D.J. (2011). Detecting spatial connections within a dendrochronological network on Vancouver Island, British Columbia. *Dendrochronologia*, 29, 49-54. doi:10.1016/j.dendro.2010.08.002

- Nijssen, B., O'Donnell, G.M., Hamlet, A.F., & Lettenmaier, D.P. (2001). Hydrologic sensitivity of global rivers to climate change. *Climatic Change*, *50*, 143-175.
- Parish, R., & Thomson, S.M. (1948-). *Tree Book: Learning to Recognize Trees of British Columbia*. British Columbia: Canadian Forest Service & B.C. Ministry of Forests.
- Pederson, G.T., Betancourt, J.L., & McCabe, G.J. (2013). Regional patterns and proximal causes of the recent snowpack decline in the Rocky Mountains, U.S. *Geophysical Research Letters*, *40*, 1811-1816. doi:10.1002/grl.50424
- Pederson, G.T., Gray, S.T., Woodhouse, C.A., Betancourt, J.L., Fagre, D.B., Littell, J.S., Watson, E., Luckman, B.H., & Graumlich, L.J. (2011). The unusual nature of recent snowpack declines in the North American Cordillera. *Science*, *333*, 332-335. doi:10.1126/science.1201570
- Peterson, D.W., & Peterson, D.L. (2001). Mountain hemlock growth responds to climatic variability at annual and decadal time scales. *Ecology*, *82*, 3330-3345.
- Peterson, D.W., Peterson, D.L., & Ettl, G.J. (2002). Growth responses of subalpine fir to climatic variability in the Pacific Northwest. *Canadian Journal of Forest Research*, *32*, 1503-1517. doi:10.1139/X02-072
- Peterson, D.W., & Peterson, D.L. (1994). Effects of climate on radial growth of alpine conifers in the North Cascade Mountains. *Canadian Journal of Forest Research*, *24*, 1921-1932.
- Pitman, K.J., & Smith, D.J. (2013). A dendroclimatic analysis of mountain hemlock ring-width and maximum density parameters, southern British Columbia Coast Mountains, Canada. *Dendrochronologia*, *31*, 165-174. doi:10.1016/j.dendro.2013.05.002
- Pojar, J., Klinka, K., & Meidinger, D.V. (1987). Biogeoclimatic ecosystem classification in British Columbia. *Forest Ecology and Management*, *22*, 119-154.
- Starheim, C.C.A., Smith, D.J., & Prowse, T.D. (2013). Dendrohydroclimate reconstructions of July-August runoff for two nival-regime rivers in west central British Columbia. *Hydrological Processes*, *27*, 405-420.
- Stewart, I.T. (2009). Changes in snowpack and snowmelt runoff for key mountain regions. *Hydrological Processes*, *23*, 78-94. doi:10.1002/hyp.7128
- Stewart, I.T., Cayan, D.R., & Dettinger, M.D. (2005). Changes toward earlier streamflow timing across Western North America. *Journal of Climate*, *18*, 1136-1155.

- Stokes, M.A., & Smiley, T.L. (1968). *An Introduction to Tree-Ring Dating*. Chicago: IL. University of Chicago Press.
- Timilsena, J., & Piechota, T. (2008). Regionalization and reconstruction of snow water equivalent in the upper Colorado River basin. *Journal of Hydrology*, 352, 94-106. doi:10.1016/j.jhydrol.2007.12.024
- Vaganov, E.A., Hughes, M.K., Kirilyanov, A.V., Schweingruber, F.H., & Silkin, P.P. (1999). Influence of snowfall and melt timing on tree growth in subarctic Eurasia. *Letters to Nature*, 400, 149-151.
- Wang, T., Hamann, A., Spittlehouse, D.L., Murdock, T.Q. (2012). ClimateWNA - High-resolution spatial climate data for Western North America. *Journal of Applied Meteorology and Climatology*, 51, 16-29. doi:10.1175/JAMC-D-11-043.1
- Watson, E., & Luckman, B.H. (2016). An investigation of the snowpack signal in moisture-sensitive trees from the southern Canadian Cordillera. *Dendrochronologia*, 38, 118-130.
- Whitfield, P.H., Moore, R.D., Fleming, S.W., & Zawadzki, A. (2010). Pacific Decadal Oscillation and the hydroclimatology of western Canada - Review and prospects. *Canadian Water Resources Journal*, 35, 1-28.
- Wigley, T.M.L., Briffa, K.R., Jones, P.D. (1984). On the average value of correlated time series, with applications in dendroclimatology and hydrometeorology. *Journal of Climate and Applied Meteorology*, 23, 201-213.
- Woodhouse, C.A. (2003). A 431-Yr reconstruction of western Colorado snowpack from tree-rings. *Journal of Climate*, 16, 1551-1561.
- Woodhouse, C.A., & Lukas, J.J. (2006). Multi-century tree-ring reconstructions of Colorado streamflow for water resource planning. *Climatic Change*, 78, 293-315. doi:10.1007/s10584-006-9055-0
- Woodhouse, C.A., Meko, D.M., MacDonald, G.M., Stahle, D.W., & Cook, Edward, R. (2010). A 1,200-year perspective of 21st century drought in Southwestern North America. *PNAS*, 107, 21283-21288. doi:10.1073/pnas.0911197107
- Yadav, R.R., & Bhutiyani, M.R. (2013). Tree-ring-based snowfall record for cold arid western Himalaya, India since A.D. 1460. *Journal of Geophysical Research: Atmospheres*, 118, 7516-7522. doi:10.1002/jgrd.50583
- Yarie, J. (1980). The role of understory vegetation in the nutrient cycle of forested ecosystems in the Mountain Hemlock Biogeoclimatic Zone. *Ecology*, 61, 1498-1514.